Parallel Session 18

Jets and Fragmentation

Organiser

S. L. Olsen *(Rochester)*

Properties of Hadronic Z^0 Decays and Test of QCD Generators

The ALEPH Collaboration
presented by K.M.Smith,
CERN and University of Glasgow, Scotland

Abstract

Global and inclusive variable distributions of 50000 hadronic Z^0 decays are used to fit the parameters of Monte Carlo QCD/hadronisation models at $\sqrt{s} = 91GeV$. Lower energy behaviour predicted from the fitted values is compared with experimental data.

1. Introduction

This analysis of 50000 Z^0 hadronic decays taken by the ALEPH detector during the first year of LEP running extends a previous analysis, [1], by more than an order of magnitude increase in the number of events, and by consideration of a larger number of global event variables. The variables x_p, $p_{\perp_{in}}$, $p_{\perp_{out}}$, S, A, T and Minor are used to fit to our data the Lund Parton Shower (PS) and Matrix Element (ME) models [2][4], in the program JETSET 7.2, and the Webber-Marchesini PS model [3], in the programs HERWIG 3.4 and 4.1. The predictions of the fitted models are then compared with data from PETRA, PEP and TRISTAN.

2. The ALEPH Detector

Details of the ALEPH detector are given in [5]. This analysis uses charged particle tracks measured by the Time Projection Chamber (TPC) and Inner Tracking Chamber (ITC) with a typical momentum resolution of $\delta p/p^2 \approx 0.001$ (GeV/c)$^{-1}$ for $p > 4$ (GeV/c) and a track finding efficiency estimated from Monte Carlo to be $(98 \pm 2)\%$ for this analysis. The trigger, requiring energy deposition in the electromagnetic calorimeter or a penetrating particle detected by associated hadron calorimeter and ITC hits, was practically 100% efficient for hadronic events.

3. Event Selection

Tracks required at least four TPC coordinates, a polar angle in the range $20^\circ < \theta < 160^\circ$, a transverse momentum $p_\perp \geq 200$ MeV/c and extrapolation to within 2 cm of the beam axis and within 5 cm of the origin in the beam direction. Hadronic events required at least five accepted tracks and a total charged energy of at least 15 GeV. Selecting the polar angle of the sphericity axis, θ_{sph}, in the range $35^\circ \leq \theta_{sph} \leq 145^\circ$ ensured that the event was well contained in the detector. Final results are not sensitive to variation of the selection criteria. The largest background, from $e^+e^- \rightarrow \tau^+\tau^-$, is estimated to be 0.25% of the accepted events. Event-shape distributions were corrected as follows for geometrical acceptance, detector efficiency and resolution, decays, missing neutrals, secondary interactions and initial state photon radiation. A first set of hadronic events was generated using the Lund PS model, including initial state photon radiation, and passed through the detector simulation program to produce simulated raw data. These were processed through the same reconstruction and analysis programs as the real data. A second Monte Carlo sample was generated without detector simulation, in which all particles with mean lifetime less than 1 ns were required to decay, all others were treated as stable, and initial state radiation was turned off. A bin by bin correction factor was then obtained by comparing the two Monte Carlo distributions. These factors were used to correct the experimentally measured distributions back to a well defined c.m. energy and final state particle composition that can be compared directly to QCD model calculations. The correction factors are typically in the range 0.9 -1.1, and in all cases between 0.5 and 1.8.

In fact, two types of correction factors were applied to the data, correcting the raw charged particle data back either to the original distributions for charged particles only, or to those for charged plus neutral particles. The plots of ALEPH event variables contain the former. By varying the simulated data to introduce shifts in track angles and momenta, increased momentum smearing and loss of track coordinates, systematic uncertainties were shown to be smaller than or comparable to the statistical errors. The influence of the event generator was studied using the Lund PS and ME models, and found to be small compared to the statistical errors. Error bars shown on the plots for ALEPH data are statistical only.

4.Fits of Model Predictions

The JETSET 7.2 PS option was fitted with and

without the $O(\alpha_s)$ modification to match the first perturbative branching to the exact first-order QCD formula. The transition from partons to hadrons is modelled by the Lund colour string approach. The parameters adjusted to fit the data were Λ_{LL}, the QCD scale parameter, M_{min}, the mass parameter used to terminate the parton shower, σ, the Gaussian width of the primary hadron transverse momentum distribution and b, the mass dependence parameter in the Lund symmetric fragmentation function for hadrons composed of u,d and s quarks. The a parameter in this function was left at its default value because it is strongly correlated with b. For the fragmentation of charm and bottom hadrons, we use the Peterson function [7], with $\epsilon_c = 0.020$ and $\epsilon_b = 0.015$ defined by data from PETRA/PEP [8]. All other parameters are left at their default values.

In the JETSET 7.2 ME option, we use the Zhu implementation of the exact ERT second order matrix element calculation [9] with $y_{min} = 0.01$. Experimental 2-, 3- and 4-jet rates at small values of the jet resolution parameter [10][11] suggest that the renormalisation mass μ be set to a very small fraction of the c.m. energy, $\mu^2 = 0.002s$, instead of $\mu^2 = s$. Both of these possibilities were fitted to our data for comparison. String hadronisation is again used, but with the fragmentation parameters a, ϵ_c and ϵ_b set to values 1.0, 0.55 and 0.012, respectively, from lower energy data. The fit parameters are again Λ_{MS}, σ and b.

HERWIG was the original model to describe the coherent LLA parton shower, now found also in Lund PS, but using a different formulation of the kinematics. No matching to the first order matrix element is done at the first branching, however. Hadronisation differs from JETSET in that all final state gluons first split non-perturbatively into $q\bar{q}$ pairs, adjacent pairs are combined into colourless clusters and finally each cluster decays into two hadrons or hadron resonances. There are no adjustable fragmentation parameters. The differences in physics content between versions 3.4 and 4.1 are small. The parameters tuned to fit the data are Λ_{LL}, the QCD scale parameter, M_G, the minimum virtual gluon mass used to terminate the parton shower and M_{CL}, the maximum allowed cluster mass. If this mass is exceeded, the cluster is split into two clusters of lower mass.

The parameters of all the models were tuned at 91.25 GeV, using the data distributions corrected for charged tracks only, and optimising the description of the global properties of the hadronic final state using x_p, $p_{\perp_{out}}$, $p_{\perp_{in}}$, Sphericity, Aplanarity, Thrust and Minor. The multi-dimensional fitting method took the correlations between parameters into account as follows. The Monte Carlo generators were run at various points in parameter space and the above distributions calculated from charged particles (without detector simulation). The dependence on the parameters of the content of each bin of each distribution was approximated by a second order Taylor polynomial, with $N_c = 1 + n + n(n+1)/2$ coefficients, where n denotes the dimension of the parameter space.

Exactly $N_c - 1$ points were randomly distributed on the surface of a n-dimensional hypersphere with unit radius, such that their mutual separations were as large as possible. The centre of the hypersphere was taken as the remaining point. The normalised coordinates of the points were then linearly mapped onto the parameter regions actually chosen.

The best fit parameter values, their errors and correlations were found by minimising the sum of χ^2's between the data and the parametrized model predictions, using the program MINUIT [12]. In our applications, 3 or 4 parameters are fitted simultaneously. At the best fit position, the Monte Carlo statistical errors were always more than 4 times smaller than the data errors, and they have been neglected in the fitting process.

5. Discussion of Results

Table 1 gives the best fit values, with errors which are statistical only but include correlations calculated by MINUIT. Table 1 also shows the χ^2 values for each distribution and for each model. Figure 1 shows the data (as points) with the predictions of the tuned models superimposed.

The best overall description of the data is given by JETSET PS, with $O(\alpha_s)$ correction, as shown in Table 1. Only in the region $p_{\perp_{out}} > 1$ GeV/c is the model somewhat low. Consequently, the values Λ and b change if either $p_{\perp_{out}}$ or $p_{\perp_{in}}$ is omitted from the set of fitted distributions. Differences between our optimised parameter values and default values based on fits to MARK II data at 29 GeV [13] include the QCD scale Λ, which is lower than the default. The infra-red stability of the Lund string model results in little sensitivity to the shower cut-off parameter M_{min}, in contrast to HERWIG.

As shown in Table 1, without the first order QCD modification of the first LLA branching there is a substantial reduction of Λ, as expected, and the fit quality is slightly worse.

The HERWIG model fits the data less well than

JETSET, mainly in that the peaks of the event shape distributions are predicted to be broader than in the data. The HERWIG predictions also fall below the data in the regions of high $p_{\perp_{in}}$(> 2 GeV) and high Feynman x (>0.6) The $p_{\perp_{out}}$distribution is better represented than by JETSET, however. The best fit values for Λ and for M_{CL} are quite distinct from their default values. The correlations between parameters are somewhat less important than in JETSET.

The ME option of JETSET 7.2 with the standard choice of renormalisation scale gives a poor description of the data, despite the tuning of 3 parameters. A large improvement in χ^2 is achieved using a renormalisation scale $\mu^2 = 0.002$ s, (cf. Table 1). The smallness of the mass scale μ^2 leads to the rather high value of 0.20 for $\alpha_s$evaluated at this μ^2.

6. Comparison with Lower Energy Data

The consistency of the QCD model predictions was tested by comparing their energy evolution with lower energy data [13] [14]. Figure 2 shows the average data values (points) and the expectations from parton shower model fit parameters tuned at the Z^0 energy. While the energy dependence of the mean Sphericity, Aplanarity, (1 - Thrust) and Minor is quite well reproduced by both models, the predicted $< p_T >$ values agree with the MARK II values, but are systematically lower than the TASSO values by about 20 MeV.

7. Charged Multiplicity

The true charged particle multiplicity was unfolded from the experimental distribution. Monte Carlo simulation was used to evaluate the matrix elements G_{ik} relating the measured population in multiplicity bin i, n_i, to the value m_k in bin k of the true distribution, via $n_i = \Sigma G_{ik} m_k$. The 'Method of Reduced Entropy' [15] was used to reduce the sensitivity of the results to fluctuations in G_{ik} values. This scheme requires the minimisation of $F = w\chi^2 - S$, with w is a positive weight factor and $S = -\Sigma_k p_k ln p_k$, with $p_k = (m_k/\Sigma_k m_k)$. The deconvoluted charged multiplicity, shown in Figure 3, gives a mean value of 20.83 ± 0.45.

References

[1] D.Decamp et al., Phys.Lett.**B234** (1990) 209

[2] M. Bengtsson and T. Sjöstrand, Phys. Lett. **185B** (1987) 435

[3] G. Marchesini and B.Webber, Cavendish-HEP-88/7 (1988);
G. Marchesini and B. Webber, Nucl. Phys. **B310** (1988) 461;
I. Knowles, Nucl. Phys. **B310** (1988) 571

[4] T. Sjöstrand and M. Bengtsson, Comput. Phys. Commun. **43** (1987) 367

[5] D.Decamp et al., Nucl. Instr. Meth.**A294** (1990) 121

[6] T.Sjöstrand et al., in *Proceedings of the Workshop on Z Physics at LEP*,, eds. G.Altarelli, R.Kleiss and C.Verzegnassi, CERN Report 89-08 Vol. 3.

[7] C.Peterson et al., Phys.Rev.**D27** (1983) 105

[8] J.Chrin et al., Z.Phys.**C36** (1987) 163;
W.Bartel et al., Z.Phys.**C33** (1987) 339;
S.Bethke, Z.Phys.**C29** (1985) 175; preprint HD-PY 86/07 (1986)

[9] R.K. Ellis, D.A. Ross and A.E.Terrano, Nucl. Phys. **B178**(1981)429

[10] S. Bethke, Z. Phys.**C43** (1989) 331

[11] M.Z. Akrawy et al., CERN-EP/89-153;
P. Abreu et al., CERN-EP/90-89;
B. Adeva et al., L3 Preprint #011

[12] CERN Program Library D506

[13] A.Petersen et al., Phys.Rev.**D37** (1988) 1

[14] I.H.Park et al., Phys.Rev.Lett. **62** (1989) 1713

[15] M. Schmelling, Z.Phys.**C40** (1988) 207

[16] Z.Koba et al., Nucl.Phys.**B40** (1972) 317

[17] W.Braunschweig et al., Z.Phys.**C45** (1989) 1939;
M.Derrick et al., Phys.Rev.**D34** (1986) 3304

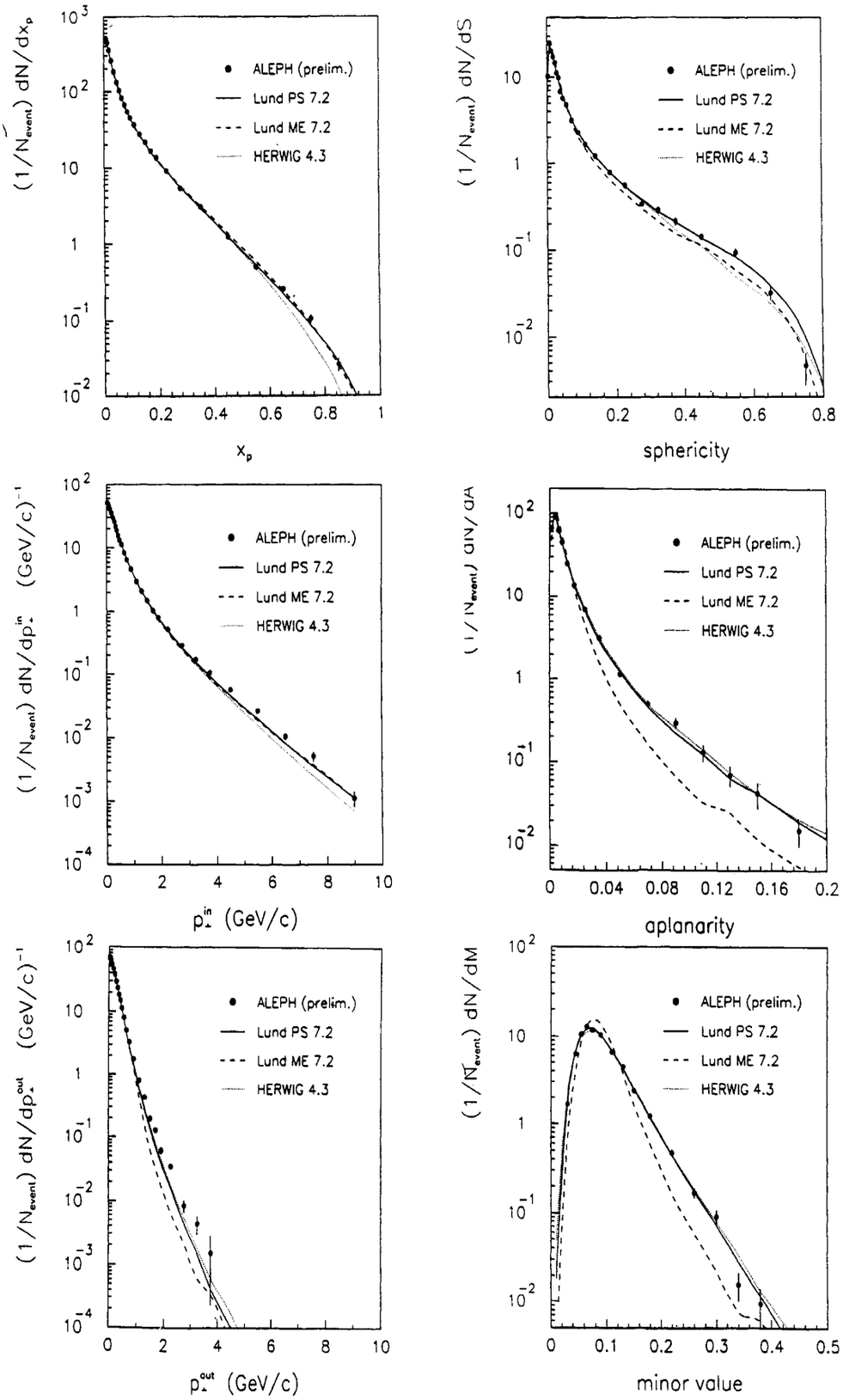

Figure 1: Comparison of ALEPH data with best fit Monte Carlo predictions.

			Distribution	x_p	$p_{\perp out}$	$p_{\perp in}$	S	A	T	M	*Sum*
			No.of bins	23	22	28	22	15	21	16	147
Model	Param.	Def.	Best Fit	Corr.							
JETSET 7.2	Λ	0.40	0.298 ± 0.008	0.92	43	88	51	15	12	16	23	248
with $O(\alpha_s)$	M_{min}	1.00	1.500 ± 0.120	0.92								
correction	σ	0.35	0.367 ± 0.004	0.89								
	b	0.90	0.890 ± 0.040	0.97								
JETSET 7.2	Λ		0.184 ± 0.006	0.90	45	104	60	22	15	42	39	327
no $O(\alpha_s)$	M_{min}	1.00	1.300 ± 0.210	0.94								
correction	σ	0.35	0.393 ± 0.004	0.89								
	b	0.90	0.650 ± 0.030	0.97								
HERWIG 3.4	Λ	0.20	0.100 ± 0.002	0.56	89	35	87	54	33	95	80	473
	M_G	0.65	0.841 ± 0.017	0.71								
	M_{CL}	5.00	3.810 ± 0.040	0.75								
HERWIG 4.1	Λ	0.20	0.094 ± 0.002	0.64	84	40	103	54	35	93	86	496
	M_G	0.65	0.813 ± 0.016	0.82								
	M_{CL}	5.00	3.940 ± 0.050	0.84								
JETSET 7.2	$\Lambda_{\overline{MS}}$		0.252 ± 0.007	0.70	171	521	138	167	285	614	347	2243
M.E.	σ	0.40	0.469 ± 0.002	0.63								
$\mu^2 = s$	b	0.70	0.414 ± 0.005	0.77								
JETSET 7.2	$\Lambda_{\overline{MS}}$		0.152 ± 0.003	0.78	180	104	64	22	21	169	26	585
M.E.	σ		0.437 ± 0.003	0.75								
$\mu^2 = 0.002s$	b		0.525 ± 0.007	0.84								

Table 1: Fitted parameter values, global correlations and χ^2 contributions from the distributions.

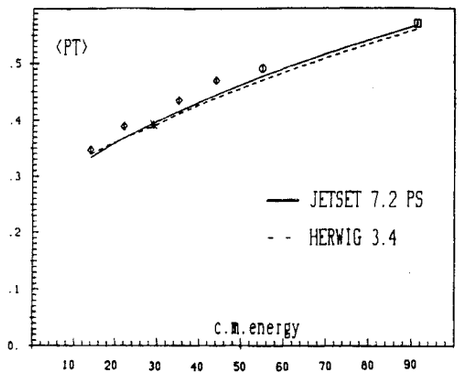

Figure 2: Energy dependence of data and predictions of HERWIG and JETSET, tuned at Z^0 energy.

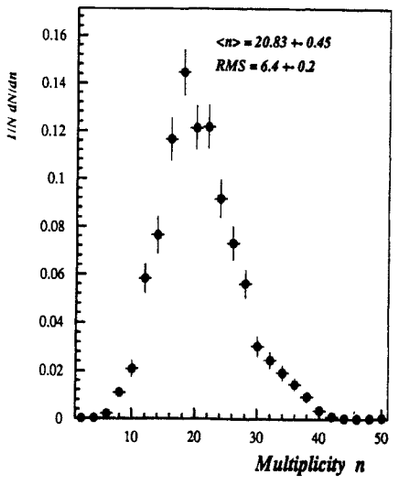

Figure 3: Unfolded charged particle multiplicity distribution.

QCD STUDIES WITH THE OPAL DETECTOR AT LEP

Robert V. Kowalewski
Physics Department, Carleton University
Ottawa, Ontario, K1S5B6, Canada

representing the OPAL Collaboration

ABSTRACT

We present results obtained using data collected with the OPAL detector during the 1989 and 1990 LEP runs. We compare several widely-used QCD Monte Carlo generators with our data on global event shapes and find the parton shower programs describe the data well. We extract $\alpha_S(M_{Z^0})$ from jet production rates and energy-energy correlations. Angular distributions in four-jet events are studied and found to be consistent with the QCD expectations, but not with an alternative model in which the triple-gluon vertex doesn't exist. We also present an analysis of the inclusive hadron momentum spectrum which suggests the need for some coherence phenomenon in the parton branching process, as is embodied by QCD.

Introduction

The hadronic decays of the Z^0 provide a good laboratory for testing the predictions of Quantum Chromo-Dynamics and measuring the coupling constant, α_S, of the theory. We discuss here the comparison of OPAL data with both analytic and Monte Carlo predictions of QCD. We begin by evaluating the quality of the description of multihadronic Z^0 decays by several widely-used Monte Carlo programs via an examination of the global properties of these events. We then discuss the determinations of $\alpha_S(M_{Z^0})$ from the OPAL data using two different techniques. The compatability of QCD predictions for jet-jet angular correlations in 4-jet final states is then presented. We conclude with a comparison of the soft hadron momentum distribution with the analytic predictions of QCD under the conjecture of Local Parton-Hadron Duality.

Global Event Shapes

OPAL has measured global event shape distributions from hadronic decays of the Z^0[1]. We compare our data with the predictions of four QCD Monte Carlo programs: Jetset 7.2[2], Herwig 3.4[3], and Ariadne 3.1[4], which generate parton showers in the leading-logarithm approximation, and with an implementation[5] of the ERT[6] second-order matrix element equations. We tune the parameters of these Monte Carlos using two shape distributions and examine the quality of the description of other distributions.

The OPAL detector has two independent subcomponents which provide good position and energy resolution over a large solid angle. The Jet Chamber, a 160 layer tracking device extending from 25 to 185cm in radius, situated inside an axial magnetic field of 4.35kG, measures charged particles over 96% of 4π. The electromagnetic calorimeter, a lead glass array, covers 98% of 4π. The barrel region consists of 9440 blocks, 25 radiation lengths deep, and each endcap has 1132 blocks of 20 radiation lengths. The efficiency for triggering and selecting multihadronic Z^0 decays is close to 100% and introduces negligible uncertainties into the analyses presented here.

The distributions obtained from the calorimeter are corrected for the effects of finite experimental acceptance and resolution, for initial state QED radiation, and for unmeasured particles (e.g., neutrinos). The correction is made bin-by-bin, and the bin sizes are chosen to correspond to the experimental resolution in the quantity under consideration. The correction factors are based on a comparison of Jetset events before and after a detailed simulation of the OPAL detector. The uncertainty in these factors is estimated by repeating the procedure using events generated with Herwig. After correction the data can be compared directly with the generated hadron distributions from the QCD Monte Carlos, and with acceptance corrected distributions from other experiments.

We use two distributions to tune the Monte Carlos: thrust major, which is sensitive to 3-jet structure, and the ratio of the second to the ze-

roeth Fox-Wolfram moment (H2/H0), which measures the isotropy of an event. The tuned parton-shower Monte Carlos give a good description of our data in all shape distributions; the matrix element Monte Carlo describes 3-jet dominated quantities well, but does less well in 2-jet dominated regions. The tuned parton shower Monte Carlos also describe data at lower center-of-mass energies well. Since the tuning procedure involved no constraints on the charged particle multiplicity we can make an unbiased comparison between our data and the Monte Carlo predictions for this quantity. We obtain an acceptance-corrected charged multiplicity of $< N_{ch} >= 21.28 \pm 0.04 \pm 0.84$, where the first error is statistical and the second systematic. The corresponding values for Jetset, Herwig, and Ariadne are 21.4, 21.2, and 20.9, respectively. The second-order matrix element Monte Carlo predicts $< N_{ch} >= 19.1$, somewhat below our value.

Determining the Strong Coupling Constant

We employ two methods for determining α_S. The first relies on measuring the production rates of 2 and 3-jet events. The second uses all measured final state particles to form two quantities, the energy-energy correlation (EEC) and its asymmetry ($AEEC$), which are sensitive to α_S.

Jet Production Rates

At LEP energies one observes jets of hadrons in the final state which reflect the underlying parton dynamics. The number of distinct jets in an event is related to the number of hard, acollinear partons, and is sensitive to α_S. To measure α_S, however, one must make a correspondence between jets and partons. We define jets using algorithms similar to the invariant mass method introduced by the JADE collaboration[7]. In this approach a particle is included in a jet if the invariant mass between the particle and the jet is smaller than a specified threshold, which is normally defined in terms of the scaled variable

$$y_{cut} = \frac{M^2_{min}}{E^2_{cm}}.$$

This process is repeated until all particles in an event have been grouped into jets. In our analysis we apply the same algorithm to partons generated in the Monte Carlo, since partons too close to be resolved into separate jets must be treated as a single parton. The procedure for combining partons is not, however, uniquely defined, since one cannot conserve energy and momentum while maintaining massless partons, as is relevant for QCD calculations. We thus consider four different schemes for combining unresolvable partons in our analysis.

Table 1: Fitted values for $\alpha_S(M_{Z^0})$ from the differential 2-jet production rate.

Fit	recombination scheme			
type	E0	E	p0	p
$f = 1$	0.125	0.143	0.121	0.120
fitted f:				
α_S	0.111	0.110	0.115	0.116
f	0.0052	0.00006	0.09	0.19
$< \alpha_S >$	0.118	0.126	0.118	0.118
	± 0.009	± 0.014	± 0.008	± 0.008

The jet finding uses both charged tracks and neutral clusters. As in the event shape analysis, we unfold the data for acceptance and initial-state radiation. Furthermore, we correct the data for the effects of hadronisation. This procedure is justified by the fact that the hadronisation corrections at $\sqrt{s} = M_{Z^0}$ are small, and that the parton shower Monte Carlos provide good descriptions of data taken over a wide energy range with a single parameter set. The uncertainties in the procedure are estimated by comparing the correction factors obtained with Jetset and Herwig, which use quite different algorithms for hadronisation, and taking the difference as the systematic error.

We fit the differential 2-jet production rate to the calculations of Kunszt and Nason[8] to obtain values for $\alpha_S(M_{Z^0})$[9]. This quantity corresponds, in each event, to the value of y at which the event classification changes from 3 to 2-jet. The bins of this distribution are statistically independent (in contrast to the jet rates themselves). Two sets of fits are performed, one in which $f = \mu^2/{E_{cm}}^2 = 1$ and α_S is the only free parameter, and a second where α_S and f are varied. Regions where 4-jet production is non-negligible are excluded from the fit, since 4-jet rates are not well described by $o({\alpha_S}^2)$ calculations, and the 2 and 3-jet rates in these regions are therefore suspect.

The fit results are given in Table 1. The first row lists the results obtained with f fixed at unity, while the second gives the values for $\alpha_S(M_{Z^0})$ and f obtained from a 2-parameter fit. The final row of the table is obtained by taking the arithmetic mean of the results for fixed and fitted f. The errors include contributions from experimental statistical and systematic errors and from theoretical uncertainties. The results from the different recombination schemes agree well, from which we conclude there is no additional uncertainty due to the choice of scheme. We therefore select the scheme which yields the most accurate value[10]:

$$\alpha_S(M_{Z^0}) = 0.118 \pm 0.008.$$

The error has contributions from the experimental statistical and systematic errors (0.003), the range of α_S between fitted f and $f = 1$, uncertainties in the hadronisation correction, and uncertainties due to the choice of the shower cutoff parameter Q0, which was varied over the range 1 GeV to 10 GeV.

Energy-Energy Correlations

The energy-energy correlation is defined as

$$EEC(\chi) = \frac{2}{\Delta\chi \cdot N} \int_{\chi-\frac{\Delta\chi}{2}}^{\chi+\frac{\Delta\chi}{2}} \sum_{evnts}^{N} \sum_{i \neq j} \frac{E_i E_j}{E_{vis}^2} \delta(\chi' - \chi_{ij}) d\chi'$$

where χ_{ij} is the angle between particles i and j and $\Delta\chi$ is the bin width for the distribution. The asymmetry is $AEEC(\chi) = EEC(\pi - \chi) - EEC(\chi)$. The 2-jet component cancels in the asymmetry, which frees $AEEC$ from some of the higher order QCD corrections important for EEC.

We form EEC and $AEEC$ using charged tracks and electromagnetic clusters, and correct these distributions bin-by-bin for the effects of experimental acceptance, initial state radiation, and hadronisation. The uncertainties in the correction procedure are estimated as in the previous analyses by comparing Jetset and Herwig-based results. We fit our unfolded data to four second-order calculations[8][12][13][14] and two matrix element Monte Carlo models[6][15] implemented in Jetset. To avoid being overly sensitive to the 2-jet dominated region, we restrict the range of angles over which we fit to $43.2° < \chi < 136.8°$ for EEC and $\chi > 28.8°$ for $AEEC$. The $\alpha_S(M_{Z^0})$ values obtained appear in Table 2. The error includes the statistical error, which is typically 0.0005 for EEC and 0.001 for $AEEC$, and the experimental systematic error, derived from comparing charged track-only and cluster-only distributions. We use the spread of the results as the theoretical uncertainty to obtain:

Table 2: Fitted values for α_S from EEC and $AEEC$.

Theory	EEC	$AEEC$
AB[12]	0.133 ± 0.006	$0.120\pm^{+0.007}_{-0.009}$
RSE[13]	0.138 ± 0.006	$0.122\pm^{+0.007}_{-0.009}$
KN[8]	0.131 ± 0.006	$0.117\pm^{+0.007}_{-0.009}$
FK[14]	0.125 ± 0.006	$0.115\pm^{+0.007}_{-0.009}$
ERT[6]	0.126 ± 0.005	$0.117\pm^{+0.007}_{-0.010}$
GKS[15]	0.133 ± 0.006	$0.118\pm^{+0.007}_{-0.010}$

$$\alpha_S(M_{Z^0}) = 0.131 \pm 0.006 \pm 0.006 \quad EEC$$
$$\alpha_S(M_{Z^0}) = 0.117^{+0.007+0.006}_{-0.009-0.002} \quad AEEC.$$

We further investigate the effect of a simultaneous adjustment of α_S and the scale factor f. The EEC prefers $f = 0.027 \pm 0.013$ at which $\alpha_S(M_{Z^0}) = 0.117$, in good agreement with the $AEEC$ value, which is insensitive to changes in f. To account for the uncertainty in the scale factor we take the mean of the values for fixed and fitted f:

$$\alpha_S(M_{Z^0}) = 0.124 \pm 0.012 \quad EEC$$
$$\alpha_S(M_{Z^0}) = 0.117 \pm 0.009 \quad AEEC.$$

The error from EEC is dominated by theory, while the error from $AEEC$ has a significant contribution from experimental systematic errors.

Four-Jet Angular Correlations

The 4-jet final states one observes in e^+e^- annihilation, in as much as they reflect 4-parton final states, are expected in QCD to have contributions from 3 processes: double gluon bremsstrahlung, $q\bar{q}$ production from a radiated gluon, and the triple-gluon vertex, where a radiated gluon decays into two gluons. The different spins of gluons and quarks lead to separate angular distributions of the partons in each case. One can attempt to discriminate between QCD and alternative theories on the basis of these angular distributions.

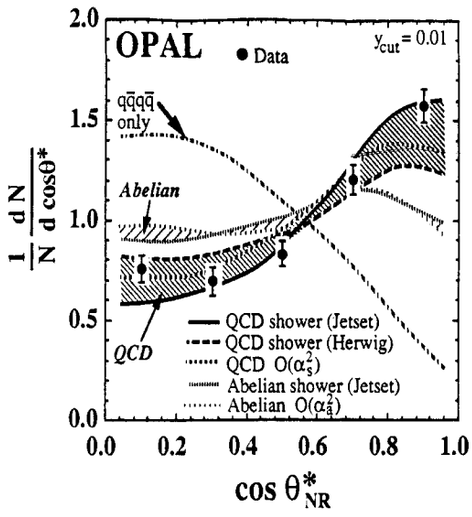

Figure 1: The measured distribution in $\cos\theta^*_{NR}$ from the OPAL data is shown along with several QCD predicitions, the predictions of the abelian vector theory, and the expectation for $q\bar{q}q\bar{q}$ final states.

We consider two measures of angular correlations in 4-jet events: χ_{BZ}[16] and $\cos\theta^*_{NR}$[17]. Jets are defined as described earlier; we consider values of y_{cut} between 0.01 and 0.04. Studies using Jetset indicate that roughly 3/4 of these observed 4-jet events exhibit 4-parton structure at identical values of y_{cut}; the remainder are predominantly misreconstructed 3-parton events. The experimental resolutions on the observables χ_{BZ} and $\cos\theta^*_{NR}$, determined using Jetset and including the effects of hadronisation, are 20° r.m.s. and 0.22 r.m.s., respectively, and exhibit a weak dependence on y_{cut}. This resolution is adequate for this analysis. Further study reveals that without experimental discrimination between quark and gluon jets the 4-quark final state can be distinguished from the $q\bar{q}gg$ states, but the diagrams producing these latter states cannot be untangled.

The experimental sample, derived from 80,200 hadronic decays of the Z^0, contains between 72 and 3880 4-jet events, depending on the choice of y_{cut} and the restrictions on jet kinematics designed at discarding background and poorly-measured events. The angular distributions we observe are consistent with the expectations of the QCD models we consider. They are: the second-order matrix element calculations and the parton shower options of Jetset, and the Herwig Monte Carlo. We find, however, that the distributions derived from either an abelian vector model, which has been implemented both in the leading-logarithm approximation and in second order perterbation theory, or from a phase space distribution of jets do not describe our data. Figure 1 shows the $\cos\theta^*_{NR}$ distribution for $y_{cut} = 0.01$. The data fall within the range of the QCD predictions, but are not well described by the abelian models. While the abelian vector model has been ruled out as a viable alternative to QCD by other measurements, the results from this analysis show that 4-jet angular correlations do provide a means to discriminate amongst alternative models. The measured mean values for χ_{BZ} and $\cos\theta^*_{NR}$ are given in table 3 along with the values expected for $q\bar{q}q\bar{q}$ final states and $q\bar{q}gg$ final states[18]. From this information we set upper limits on the fractional contribution of 4-quark final states to our sample (see table 3). The discrimination power in this analysis comes from the stringent upper limit on 4-quark final states: the upper limit of 9.1% is consistent with the 4-quark fraction of 4.7% expected from QCD, but clearly not with the 31.4% predicted by the abelian vector model.

Table 3: The measured mean values of χ_{BZ} and $\cos\theta^*_{NR}$, corrected for acceptance and hadronisation. The expectations for $q\bar{q}gg$ and $q\bar{q}q\bar{q}$ final states are also given, from which we derive upper limits on the fraction of 4-parton events coming from $q\bar{q}q\bar{q}$ final states.

	$< \chi_{BZ} >$	$< \cos\theta^*_{NR} >$
measured	43.47 ± 0.70	0.579 ± 0.008
$q\bar{q}q\bar{q}$	54.98 ± 0.20	0.388 ± 0.002
$q\bar{q}gg$	43.71 ± 0.26	0.580 ± 0.003
95% c.l. upper limit on $q\bar{q}q\bar{q}$ fraction	$< 11.8\%$	$< 9.1\%$

Coherence Effects in Soft Hadron Production

Gluon radiation in QCD occurs coherently from a $q\bar{q}$ system. This leads to destructive interference, which can be described mathematically by an angular ordering condition. Physically, this implies a reduced probability for soft gluon radiation. If we assume the number of produced hadrons

follows the number of radiated gluons, a conjecture commonly known as Local Parton-Hadron Duality[19], then we expect to observe fewer soft hadrons and therefore a lower charged multiplicity than would be produced in the absence of this destructive interference. We have compared the acceptance-corrected scaled momentum distribution ($\log(1/x_p)$) of charged particles from multihadronic Z^0 decays with QCD motivated analytic calculations[22] and Monte Carlo predictions, as well as with a model in which incoherent parton branchings and independent fragmentation are used[20]. We find the QCD calculations predict the mean of $\log(1/x_p)$ well over a range of center-of-mass energies, as do the Jetset and Herwig parton shower Monte Carlos. The model without coherence, however, cannot describe LEP data and data taken at lower energies[21] simultaneously.

Summary

The data from the first year of LEP operation have already enabled significant tests and measurements of QCD. We find $\alpha_S(M_{Z^0})$ to be 0.118 with an accuracy of about 7% using two different measuring techniques. Studies of the $\log(1/x_p)$ spectrum and 4-jet angular correlations show agreement with QCD predictions, and can discriminate against non-QCD alternatives. The accuracy of many of the measurements is limited by theory; however, higher statistics data samples will enable more selective tests of QCD at LEP in the future.

References

[1] OPAL Collab., *Z. Phys.* **C47** (1990) 505.

[2] T.Sjöstrand, *Comp. Phys. Comm.* **39** (1986) 347; T.Sjöstrand and M.Bengtsson, *Comp. Phys. Comm.* **43** (1987) 367.

[3] G.Marchesini and B.R.Webber, *Nucl. Phys.* **B310** (1988) 461.

[4] U.Pettersson, LU TP 88-5 (1988); L.Lönnblad and U.Pettersson, LU TP 88-15 (1988); L.Lönnblad, LU TP 89-10 (1988).

[5] N.Magnussen, Wuppertal Ph.D. Thesis, WUB-DI 88-4 (1988).

[6] R.K.Ellis, D.A.Ross and A.E.Terrano, *Nucl. Phys.* **B178** (1981) 421.

[7] JADE Collab., W.Bartel *et al.*, *Z. Phys.* **C33** (1986) 23; JADE Collab., S.Bethke, *et al.*, *Phys. Lett.* **B213** (1988), 235.

[8] Z.Kunszt and P.Nason [conv.], in *"Z Physics at LEP 1"* (eds. G.Altarelli, R.Kleiss and C.Verzegnassi), CERN 89-08 (1989).

[9] OPAL Collab., *Phys. Lett.* **B235** (1990) 389.

[10] OPAL Collab., CERN-PPE/90-143 (1990), *to be published in Z. Phys.*

[11] OPAL Collab., CERN-PPE/90-121 (1990), *to be published in Phys. Lett.* **B**.

[12] A.Ali and F.Barreiro, *Phys. Lett.* **B118** (1982) 155; *Nucl. Phys.* **B236** (1984) 269.

[13] D.G.Richards, W.J.Stirling and S.D.Ellis, *Phys. Lett.* **119B** (1982) 193; *Nucl. Phys.* **B229** (1983) 317.

[14] N.K.Falck and G.Kramer, *Z. Phys.* **C42** (1989) 459.

[15] F.Gutbrod, G.Kramer and G.Schierholz, *Z. Phys.* **C21** (1984) 235.

[16] M.Bengtsson and P.Zerwas, *Phys. Lett.* **B208** (1988) 306.

[17] O.Nachtmann and A.Reiter, *Z. Phys.* **C16** (1982) 45.

[18] OPAL Collab., CERN-EP/90-97 (1990), *to be published in Z. Phys.*

[19] D.Amati and G.Veneziano, *Phys. Lett.* **B83** (1979) 87; Ya.I.Azimov, Yu.L.Dokshitzer, V.A.Khoze and S.I.Troyan, *Z. Phys.* **C27** (1985) 65.

[20] OPAL Collab., *Phys. Lett.* **B248** (1990) 617.

[21] TASSO Collab., W.Braunschweig et al., DESY 90-013.

[22] Yu.L.Dokshitzer and S.Troyan, Leningrad preprint LNPI 922 (1984); Yu.L.Dokshitzer, V.A.Khoze, A.H.Mueller and S.I.Troyan, *Rev. Mod. Phys.* **60** (1988) 373; C.P.Fong and B.R.Webber, *Phys. Lett.* **B229** (1989) 289.

DISCUSSION

Q. **M. Ciaraloni** *(INFN, Firenze)*: Do you have any results on the multiplicity dispersion, and do they show KNO scaling? I am asking because QCD predicts some slow varying deviations from KNO scaling.

A. **R. Kowalewski**: We have no results on KNO scaling at this time.

Q. **M. Jacob** *(CERN)*: What would you now consider the most precise approach to $\alpha_s(M_Z)$, the 3 jet direct analysis on the AEEC analysis?

A. **R. Kowalewski** *(CERN)*: At some level that's a matter of taste. The jet rate value includes the largest range of systematic uncertainties in the quoted error.

DELPHI RESULTS ON MULTIPLICITY, INTERMITTENCY AND TRIPLE-GLUON VERTEX

HEINZ MÜLLER
Inst. für Experimentelle Kernphysik
Universität Karlsruhe

ABSTRACT

Results are given for hadronic events from the Z^0. The multiplicity distribution of charged particles is well described by a modified negative binominal distribution. The slope of the negative binominal coefficient $1/k$ is different for μp and e^+e^-. The multiplicity distributions show KNO-scaling. In the study of intermittency the dependence of the factorial moments on the size of the subintervals in rapidity is well described by the LUND-generators. Study of two-dimensional angular distributions of four-jet events gives evidence for the triple-gluon vertex.

The reported analyses are based on data taken with the DELPHI detector at LEP. Only charged tracks in the range $25° < \theta < 155°$ are used. The main requirements for the selection of hadronic events were: $E_{ch} = \sum E_i > 3GeV$ for each hemisphere and $> 15GeV$ for both hemispheres together, ≥ 5 tracks with momentum $\geq 0.2GeV/c$, $40°$ < polar angle of sphericity axis < $140°$. The last cut ensures that the selected events were largely contained inside the Time Projection Chamber. The largest background after our cuts was due to $\tau^+\tau^-$ events and was estimated to be around 0.24%.

1. Charged Multiplicity Distributions

The data sample for this analysis contained 2073 events after the cuts. The observed multiplicity distribution $N_{obs}(n_{obs})$ was corrected to get the true one $N_{tr}(n_{tr})$ by a unitary matrix M: $N_{tr}(n_{tr}) = \sum_{n_{obs}} M(n_{tr}, n_{obs}) N_{obs}(n_{obs})$ with coefficients $M(n_{tr}, n_{obs})$ determined by Monte Carlo events. The average charged multiplicity $\langle n_{ch} \rangle = 20.83 \pm 0.14(stat) \pm 0.96(syst)$ agrees well with the other results around 91 GeV from MARK2, ALEPH and OPAL [1]. These values together with other e^+e^- data [2] above $E_{cms} = 10GeV$ fit the energy dependences $a+b\ln(s)+c\ln^2(s)$, $a+b\exp(c\sqrt{\ln(s/Q_0^2)})$ and $a\alpha_s^b \exp(c/\sqrt{\alpha_s})$ well, where α_s is the running strong coupling constant and b,c are given by QCD. With these new LEP data it is now possible to exclude a power law dependence $\langle n_{ch} \rangle = a \cdot s^b$ with a $\chi^2 = 153/70DF$.

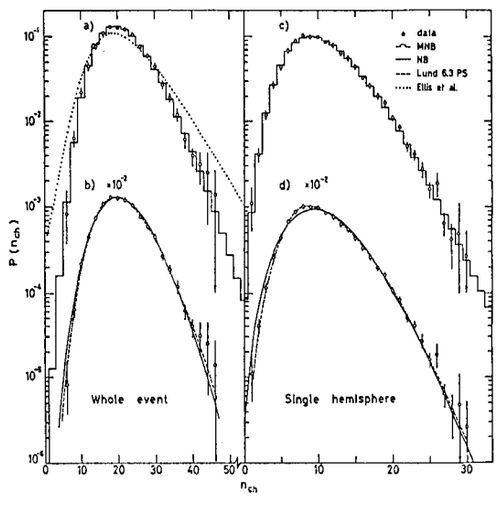

Fig. 1: Corrected charged multiplicity distributions

Comparison with Models

The JETSET 6.3 Parton shower model describes the charged multiplicity distributions (Fig.1) well for whole events and for single hemispheres. The Negative Binomial (NB) distribution: $P_n(m,k) = \frac{k(k+1)...(k+n-1)}{n!(1+m)^k}(\frac{m}{1+m})^n$ with the parameter k and $m = \langle n \rangle / k$ gives a good fit for whole events but is less good for single hemispheres. Better agreement in both distributions is achieved with a Modified Negative Binomial (MNB) characterized by the generating function $M(x) = (\frac{1+\Delta(1-x)}{1+m(1-x)})^k$, where $m = \Delta + \langle n \rangle / k$. The recent model of Ellis-Karliner-Kowalski [3] gives too broad a distribution.

Comparison with other Reactions

The NB parameter k can be parametrised in the formula $\frac{1}{k} = a + b\ln(\sqrt{s}/Q_0)$. The slope (Fig. 2) for

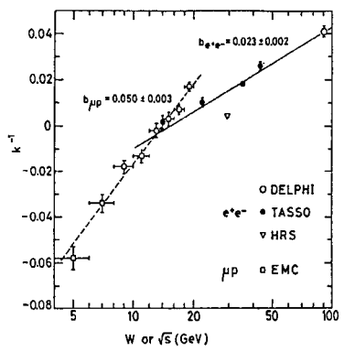

Fig. 2: Energy dependence of the NB parameter k^{-1}

$e+e-$ is only $\approx 1/2$ of that for μp reactions. This difference is now well established.

KNO-Scaling

This implies that the dependence of $\psi(z) = \langle n_{ch}\rangle P(n_{nch})$ on $z = n_{ch}/\langle n_{ch}\rangle$ is independent of energy, where $P(n_{ch})$ is the probability of an event having n_{ch} tracks. KNO-Scaling [4] is well fullfilled for whole event (Fig. 3) and single hemisphere distributions (not shown). KNO-scaling was originally derived from Feynman scaling and is now proved more generally by Chliapnikov and Tchikilev [5]. They show that it is sufficient to assume that the basic branching process is independent of energy.

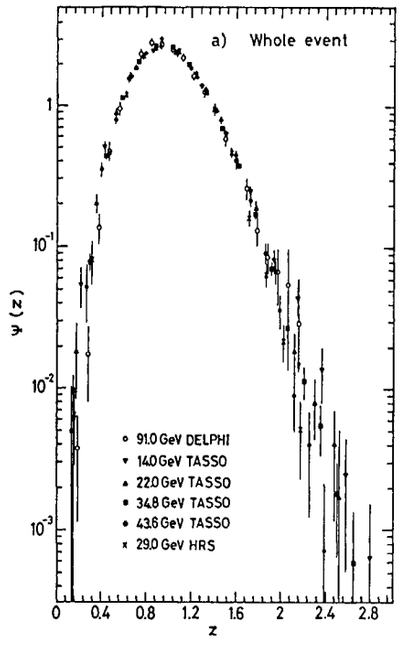

Fig. 3: KNO-scaling

2. Study of Intermittency

The term intermittency arose in the interpretation of measurements of the velocity flow and temperature spots in a turbulent medium. Theoretical work on classical systems showed that intermittency could be studied through the scaling properties of the moments of random variables in decreasing domains. For a review see [6]. A. Bialas and R. Peschanski [7] applied the method to the study of intermittency, i.e. 'sporadic spiking' in multihadron phenomena. Following their proposal we study the dependence of the factorial moments F_q of the rapidity distributions on the size $\delta y = Y/M$ of the M subintervals (range Y fixed):

$$F_q(\delta y) = \frac{M^{q-1}}{\langle N\rangle^q}\langle \sum_{m=1}^{M} N_m(n_m-1)...(n_m-q+1)\rangle$$

F_q measures the probability to have $\geq q$ particles in a δy bin. For a Poisson distribution $F_q(\delta y) \approx const.$ Variation with δy indicates fluctuations of physical origin. Selfsimilar cascade models give a power law, for example.

The DELPHI data used contain 7753 multihadron events after the cuts [8]. The factorial moments F_2 to F_5 (Fig.4) flatten off for $\delta y < 0.4$. They are well described by the default JETSET 6.3 parton shower version. They disagree with the default JETSET 7.2 matrix element version which is tuned to the PEP and PETRA data around 30 GeV. But they agree within 15% with this version after retuning the parameters to fit to the data from the Z^0. The large differences show that the factorial moments are very sensisitive to this tuning. In the DELPHI data there is no need for physics beyond that in the Lund-generators. The same conclusion has been reached in an analysis of the CELLO collaboration [9]. The TASSO collaboration [10] claims to have intermittent behavior down to their smallest δy and deviation from the prediction of the LUND-model.

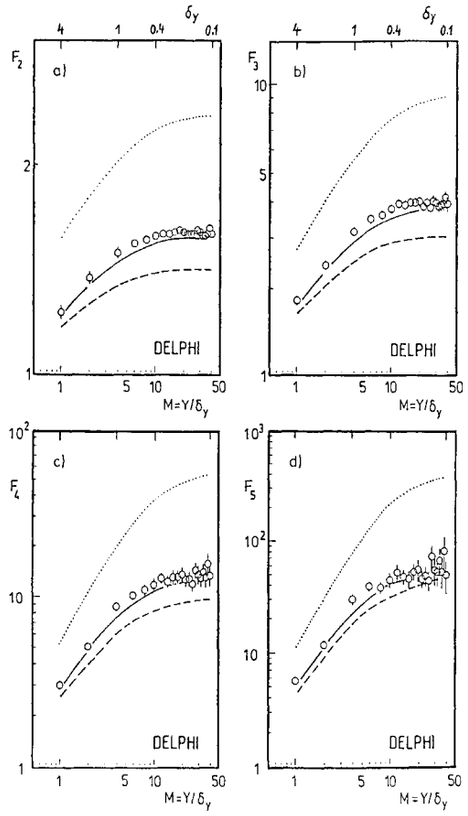

Fig. 4: Dependence of the factorial moments on the number of subdivisions of the rapidity interval (—— = Lund-PS, $\cdots$ = Lund-ME, – – – = Lund-ME retuned).

3. Evidence for the Triple-Gluon Vertex

The self-coupling of the gluons is an essential feature of QCD. It originates from the color charges of the gluons which is a direct consequence of the non-Abelian nature of this gauge theory. In e^+e^- annihilation, gluon self-coupling appears in second order QCD where one has 4-parton contributions from double bremsstrahlung, the triple-gluon vertex, and secondary $q\bar{q}$-production. If one orders the jets in four-jets events according to their energy then jet 3 and jet 4 correspond preferentially to the secondary partons.

Studying the angular distributions of four-jet events the AMY, OPAL, L3 and VENUS collaborations [11] have published evidence against a QED-like Abelian theory [12] in which the gluon is colourless and the threefold colour of the quarks is retained. The one-dimensional distributions they studied distinguish only between the triple-gluon vertex contribution and the secondary $q\bar{q}$-contribution.

As in the other publications [11] we use the generalised Nachtmann-Reiter angle θ^*_{NR} (Fig. 5), but in addition we use the angle α_{34} (Fig. 5) between the secondary jets which distinguishes between triple-gluon vertex and double bremsstrahlung.

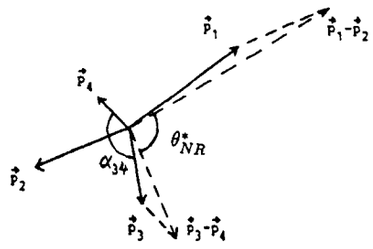

Fig. 5: Definition of θ^*_{NR} and α_{34}

Method

R.K. Ellis et al. [13] have calculated the differential cross section for the production of the four-parton final states in order α_s^2. The transition probabilities can be grouped into classes corresponding to:

A: planar graphs for double-bremsstrahlung $\propto C_F^2$
B: non-planar $\propto C_F(C_F - \frac{1}{2}N_C)$
C: graphs with the triple-gluon vertex $\propto C_F N_C$
D: planar graphs for secondary $q\bar{q} \propto C_F T_R$
E: non-planar $\propto C_F(C_F - \frac{1}{2}N_C)$
F: not relevant here $\propto C_F$

The grouping of the graphs is done in a gauge invariant way. For QCD the fermionic Casimir operator is $C_F = \frac{4}{3}$, the number of colours $N_C = 3$ and $T_R = \frac{1}{2}n_f$ where n_f stands for the number of quark flavours. For the Abelian theory one has $C_F = 1$, $N_C = 0$, $T_R = 3n_f$. The aim of the analysis is to determine the individual contributions. We take $\frac{N_C}{C_F}$ and $\frac{T_R}{C_F}$ as free variables and fit the two-dimensional distribution in $|\cos\theta^*_{NR}|$ and $\cos\alpha_{34}$ to our data.

Analysis

This analysis is based on 21024 multihadron events from Z^0 decay. The jet-algorithm LUCLUS from the JETSET-package [14] is used. With the jet resolution parameter $djoin = 5\,GeV\,\frac{E_{vis}}{E_{cms}}$ we get 884 four-jet events.

We have generated 40000 four parton events with JETSET 7.2 and passed these events through the full simulation of the DELPHI detector and the DELPHI analysis chain. From this sample the LUCLUS algorithm gives 6102 4-jet events. Then 20000 events have been generated in the Abelian theory. The simulated 4-jet sample has been checked for consistency with the 4-jet events extracted from the data. The distributions of the event-quantities thrust, $p_{t,in}$, $p_{t,out}$ and, separately for the jets 1 to 4, the jet momentum distributions and the particle distributions in p_t, p_l, N_{ch} agree within their statistical accuracy.

We sort our simulated four jet events according to their values of $|\cos\theta^*_{NR}|$ and $\cos\alpha_{34}$ in a 10 x 10 matrix. The classes A,B and D,E contribute with different factors in QCD and the Abelian theory and this allows seperation of contribution A from B and D from E. Class C is extracted directly from the QCD-events. The expected relative contributions of the groups A, B, C, D, E after simulation of the DELPHI-detector are 34%, -5%, 65%, 6%, -0.1% for QCD and 27%, 32%, 0%, 41%, 0.5% for the Abelian theory. We perform a maximum likelihood fit of the 10 x 10 matrix from the data to the theoretical distribution:

$$Theo_{l,m} = X_1 * [A_{l,m} + (1 - \tfrac{1}{2}X_2)\,B_{l,m} + X_2\,C_{l,m} + X_3\,D_{l,m} + (1 - \tfrac{1}{2}X_2)\,E_{l,m}] + P3J4_{l,m}$$

with the three variables $X_1 = Norm * C_F^2$, $X_2 = \frac{N_C}{C_F}$, and $X_3 = \frac{T_R}{C_F}$. $P3J4$ represents the 4-jet background of 4% from three and two parton events.

Results

The results of the fits are given in Table 1. Inserting for $\frac{N_C}{C_F}$ and $\frac{T_R}{C_F}$ the exact QCD values and fitting only the normalisation factor gives almost the same log-likelihood value as the free fit. In the fit with $\frac{N_C}{C_F} = 0$, in which only double bremsstrahlung and secondary quark-antiquark production contribute, the reduction of the log-likelihood value originates mainly from the observable α_{34}, as is evident from the χ^2-values of the projections in Table 1. For the specific QED-like Abelian theory in which the ratio of

Table 1: Results of the maximum likelihood fits to the 10x10 matrix in $|\cos\theta^*_{NR}|$, $\cos\alpha_{j3j4}$. The last two columns give the χ^2 for the projections.

Fit	$\frac{N_C}{C_F}$	$\frac{T_R}{C_F}$	log-L	θ^*_{NR}	α_{34}
Free	2.05 ± 0.4	0.1 ± 1.7	834.9	8.6	7.7
QCD	2.25	1.875	834.4	9.3	7.4
$g \not\to gg$	0	2.8 ± 2.3	814.6	9.6	21.1
ABEL	0	15	802.8	34.0	16.5

of these two contributions is fixed, the reduction originates mainly from the difference in θ^*_{NR}. We check that our data are well described by QCD in the projections (Fig. 6). The χ^2 for the projections in Table 1 show good agreement with the QCD predictions for both observables.

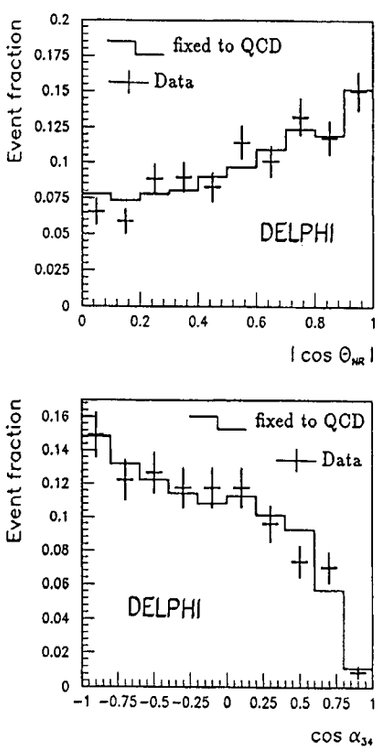

Fig. 6: Projected distributions for data and QCD

The available statistics for QCD and the Abelian theory have to be split up into the the classes A, B, C, D, E. We have determined the influence of the finite statistics of the Monte-Carlo simulation in this case empirically. With JETSET 7.2 and a simple detector simulation, 5 pairs of simulations have been generated and fitted against each other. For our finite Monte-Carlo statistics the fit results for $\frac{N_C}{C_F}$ are shifted towards smaller values. The nominal value $\frac{N_C}{C_F} = 2.25$ is reached only asymptotically with increasing statistics.

The influence of fragmentation and models has been studied similarily by comparing samples generated with different schemes. We used additionally in the matrix-element version the fragmentation parameters of JETSET 6.2 [14] which are matched to the data from PETRA and PEP in the 30 GeV region, settings for optimised scale [15], and the default parton-shower version with gluon-polarisation and interference.

Including the error and bias from the simulation and the fluctuations of the results using the different fragmentations and models we get for the final result of the free fit

$$\frac{N_C}{C_F} = 2.05 \pm 0.4(stat.)^{+0.7}_{-0.1}(simul.) \pm 0.4(fragm.)$$

which gives significant evidence for a contribution from the triple-gluon vertex.

Our thanks go to T. Sjöstrand for many helpful discussions.

References

1. MARK2 Coll., Phys. Rev. Lett. 64 (1990) 1334
   ALEPH Coll., Phys. Lett. B234 (1990) 209
   OPAL Coll., CERN-EP/90-48
2. TASSO Coll., Z. Phys. C45 (1989) 193
   ADONE Coll., Phys. Lett. B86 (1979) 234
   LENA Coll., Z. Phys. C9 (1981) 1
   MARK1 Coll., Phys. Rev. D26 (1982) 969
   CLEO Coll., Phys. Rev. Lett. 49 (1982) 357
   JADE Coll., Z. Phys. C20 (1983) 187
   HRS Coll., Phys. Rev. D34 (1986) 3304
3. J. Ellis, M. Karliner and H. Kowalski,
   Phys. Lett. B235 (1990) 341
4. Z. Koba, H.B. Nielsen and P. Olesen,
   Nucl. Phys. B40 (1972) 317
5. P.V. Chliapnikov and O.G. Tchikilev,
   Phys. Lett. B242 (1990) 347
6. Y.B. Zeldowich et.al., Sov. Phys. Usp. 30 (1987) 353
7. A. Bialas and R. Peschanski,
   Nucl. Phys. B273 (1986) 703
8. DELPHI Coll., Phys. Lett. B247 (1990) 137
9. M. Feindt this conference and DESY 90-114
10. TASSO Coll., Phys. Lett. B231 (1989) 548
11. AMY Coll., Phys. Rev. Lett. 62 (1989) 1713
    OPAL Coll., CERN-PPE/90-97
    L3 Coll., Phys. Lett. B248 (1990) 227
    VENUS Coll., KEK Preprint 90-62
12. K. J. F. Gaemers and J. A. M. Vermaseren,
    Z. Phys. C7 (1980) 81
13. R.K. Ellis, D.A. Ross and E.A. Terrano,
    Nucl. Phys. B178 (1981) 421
14. T. Sjostrand, M. Bengtsson, Comp. Phys. Comm. 43
    (1987) 367. (We use version 7.2, Nov. 1989)
15. W.de Boer et al., Univ. Karlsruhe, IEKP-KA/90-4

DISCUSSION

Q. **V. Cavasinni** *(INFN, Pisa)*: All multiplicity distributions obey KNO scaling as you also have shown. What kind of physics is behind this scaling law? Does it mean that the quark fragmentation process does not depend on energy?

A. **H. Müller**: This is an experimental result. It has been proven at the beginning to be a consequence of Feynman scaling, now there are more general arguments to prove it.

M. Ciafaloni: From the QCD point of view we do expect approximate KNO scaling as shown in our paper.

A comment on KNO scaling. In QCD the basic branching process does depend on energy because of running α_s and opening of phase space. Thus, you expect asymptotic KNO scaling, but with slowly varying deviations, as noticed long ago by Bassetto, Marchesini and myself.

Z. Fodor *(Eötvös Univ.)*: The difference between QCD and the Abelian model is about 20% if one studies the angle distribution (e.g. θ_{NR} and Y_{BZ}). This is the same order of magnitude as that for the higher order QCD corrections. Thus, these tests are far from being definitive. One has to use test less sensitive to the unknown higher order corrections.

A Test of QCD based on 4-Jet Events from Z^0 Decays

The L3 Collaboration

Patricia L. McBride
Harvard University, Cambridge MA, USA

ABSTRACT

The measured angular correlations between jets in 4-jet events from Z^0 boson decays are well reproduced by QCD. An alternative abelian model fails to describe the data. The main difference is due to the large rate of $q\bar{q}q\bar{q}$ final states in the abelian model.

Perturbative QCD [1] predicts two classes of 4-jet events in $e^+e^- \rightarrow Z^0 \rightarrow$ hadrons events;

$$Z^0 \rightarrow q\bar{q}gg \quad (1)$$
$$Z^0 \rightarrow q\bar{q}q\bar{q} \quad (2),$$

where process (1) includes the "three gluon vertex" which is a consequence of the self-coupling of the gluon. The nonabelian nature of QCD implies this self-interaction of gluons. Various tests of QCD which are sensitive to the gluon self-coupling have been proposed[2,3,4]. These tests are based on the study of angular correlations in 4-jet events. Such tests become feasible at the Z^0 resonance since the the hadronic cross section is large. We present here a study of 4,200 4-jet events observed at $\sqrt{s} \approx 91$ GeV in the L3 detector at LEP.

In QCD, the differential and total cross sections for processes (1) and (2) can be written as a linear combination of gauge invariant terms with color factors $N_C = 3$, $C_F = 4/3$ and $T_R = N_F/2 = 5/2$, where N_f is the number of quark flavors[5].

In an alternative model with 3 color degrees of freedom for the quarks, QCD′ , there is no self-coupling of the spin-1 gluons. In this abelian model, the color factors are $N'_C = 0$, $C'_F = 1$, and $T'_R = 3N_F = 15$. If α'_s for this model is chosen to be $4/3 \cdot \alpha_s$, the total cross section and the 3-jet rates are the same as in QCD up to first order[6]. However, it is important to note that QCD′ is not compatible with other measurements such as the energy dependence of jet rates [7]. Its only purpose is to provide a consistent theoretical alternative to QCD.

Figure 1 shows the generic Feynman diagrams corresponding to processes (1) and (2). In QCD′ , it is only the double Bremsstrahlung diagrams that contribute to process (1), and process (2) constitutes about 34% of the total 4-parton production cross section. In QCD, the $Z^0 \rightarrow q\bar{q}q\bar{q}$ rate is only 6%[8]. The predicted rate of process (2) ($Z^0 \rightarrow q\bar{q}q\bar{q}$) is the main difference between the models QCD and QCD′ .

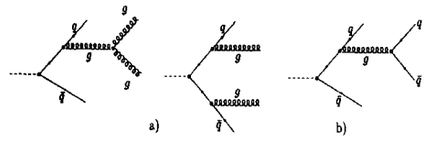

Figure 1: Generic Feynman diagrams for production of four partons in second order perturbation theory for process a) $Z^0 \rightarrow q\bar{q}gg$ and b) $Z^0 \rightarrow q\bar{q}q\bar{q}$.

The L3 Detector

The L3 detector consists of a time expansion chamber (TEC) for vertex detection, a high resolution electromagnetic calorimeter composed of BGO crystals, an array of scintillation counters, a uranium and brass hadron calorimeter with proportional wire chamber readout, and an accurate muon chamber system. These detectors are installed in a 12 m diameter magnet which provides a uniform field of 0.5 T along the beam direction. Using the calorimeters, we measure the axis of jets with an angular resolution of 2.5° and the total energy of hadronic events with a resolution of 10.2%. The

calorimeters cover 99% of 4π. A description of each detector subsystem, and its performance, is given in Reference [9].

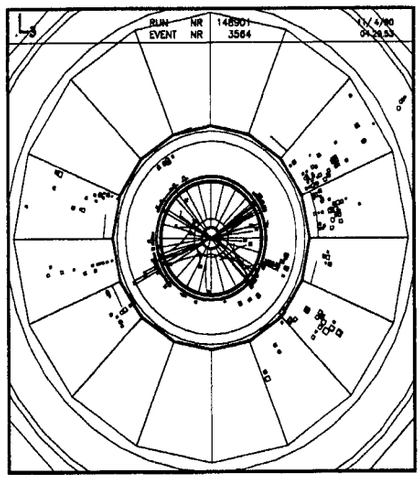

Figure 2: A 4-jet event in the L3 detector.

Figure 2 displays a reconstructed 4-jet event observed in the L3 detector. Shown are the charged tracks measured in the vertex chamber and the energy deposited in the electromagnetic calorimeter and hadron detector.

The selection of $e^+e^- \rightarrow$ hadrons events is based on the energy measured in the electromagnetic detector and the hadron calorimeter:

- $0.6 < \frac{E_{\rm vis}}{\sqrt{s}} < 1.4$
- $\frac{|E_\parallel|}{E_{\rm vis}} < 0.40$, $\frac{E_\perp}{E_{\rm vis}} < 0.40$
- $N_{cluster} > 12$

where $E_{\rm vis}$ is the total energy observed in the detector, $E_\parallel$ is the energy imbalance along the beam direction, and $E_\perp$ is the transverse energy imbalance. Neighboring calorimeter hits are grouped into clusters. The cut on the number of clusters rejects low multiplicity events (e^+e^-, $\mu^+\mu^-$, $\tau^+\tau^-$).

In total 49,000 events were selected. Applying these cuts to a sample of simulated events, we calculate an acceptance of 97% for hadronic decays of the Z^0. The contamination from e^+e^- and $\tau^+\tau^-$ final states and from $e^+e^- \rightarrow e^+e^-$ + hadrons has been found to be negligible.

Monte Carlo events are generated by the parton shower program JETSET 7.2 [10] with $\Lambda_{\rm LL}$ = 290 MeV and string fragmentation. The generated events are passed through the full L3 detector simulation [12]. The measured distributions in event shape variables and in the cut quantities agree well with the simulated distributions[13].

Analysis of 4-Jet Events

Jets are reconstructed out of clusters in the calorimeters by using the 'JADE' version [14] of an invariant mass jet algorithm. First the energy and direction of all clusters are determined. For each pair of clusters i and j the scaled invariant mass squared

$$y_{ij} = 2E_iE_j/E_{\rm vis}^2 \cdot (1 - \cos\theta_{ij})$$

is then evaluated. E_i and E_j are the cluster energies and θ_{ij} is the angle between clusters i and j. The cluster pair for which y_{ij} is smallest is replaced by a pseudocluster k with four-momentum

$$p_k = p_i + p_j \ .$$

This procedure is repeated until all y_{ij} exceed the jet resolution parameter $y_{\rm cut}$. The remaining (pseudo)clusters are called jets.

We use $y_{\rm cut}$ = 0.02, which corresponds to jet pair masses of 13 GeV or more. With this cut we are not only insensitive to the details of hadronization and heavy quark decays, but also have a large fraction (9%) of 4-jet events. In total, 4,200 4-jet events were selected. Figure 3 shows the measured energy distributions of the four energy ordered jets. These distributions are in good agreement with the Monte Carlo predictions.

Comparison to Theoretical Models

We have studied three different angular variables that describe 4-jet events and are sensitive to the differences between QCD and QCD' . To be able to compare the experimental distributions to those predicted by the theoretical models, we divide our data into 4 bins in each variable and we correct for detector effects, acceptance and resolution. To generate the theoretical predictions we use two different options in the JETSET 7.2 Monte Carlo program:

a) Matrix elements, calculated to second order in QCD ([5,15]).

b) Parton shower evolution, obtained from 'leading log' approximations.

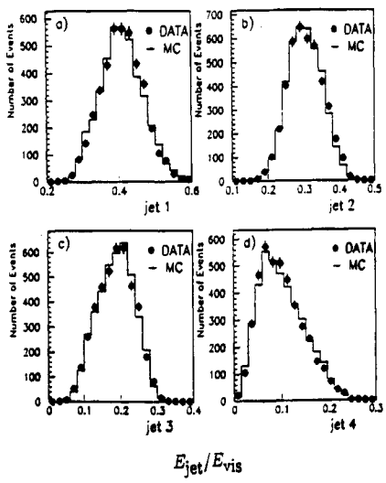

Figure 3: Measured distributions of E_{jet}/E_{vis} for energy ordered jets in 4-jet events in comparison with the Monte Carlo predictions (parton shower, Λ_{LL} = 290 MeV).

The differences between these two approaches can be considered as theoretical uncertainties [8,16]. For a) we use the value $\Lambda_{\overline{MS}} = 190$ MeV [7] and a renormalisation scale $\mu^2 = 0.08 \cdot s$ for the QCD prediction. For the abelian model, the strong coupling constant is increased with respect to QCD by a factor of 4/3. The parton shower calculations b) are performed with $\Lambda_{LL} = 290$ MeV for QCD. For the abelian shower model, we use the JETSET parameters as suggested in [8].

We have measured the fragmentation parameters by studying event shape variables and comparing the measured distributions to those predicted by the parton shower Monte Carlo and the second order matrix element generator. The uncertainty due to hadronization is estimated by changing the fragmentation parameters from the JETSET default values to the measured ones which modifies the distributions by less than 5% per bin. We have assumed the same fragmentation parameters for the abelian model as for QCD. A small correction for inital and final state radiation of about 2% per bin has been taken into account.

Our data sample contains a background of 30% from 3-jet events on the generator level which are classified as 4-jet events. We also lose a fraction of 4-jet events, however, this number is close to the number of background events, and the difference in the angular distributions for these event classes is small. Therefore, the total correction is below 3% per bin.

The distributions of the three angular variables are shown in Figures 4-5. The bands indicate the theoretical uncertainties coming from the difference between the matrix element and parton shower approaches and from hadronization uncertainties.

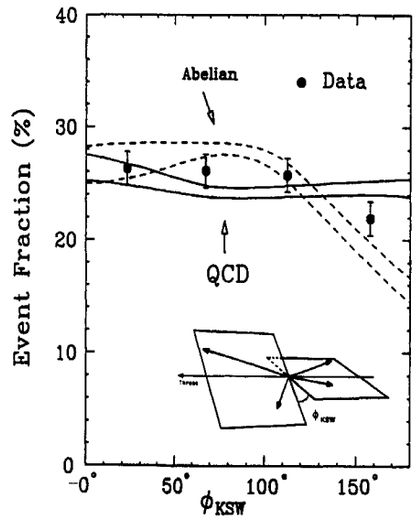

Figure 4: Measured distribution of Φ_{KSW}. The predictions for QCD and the abelian model QCD′ are shown as bands indicating the theoretical uncertainties.

The variable, Φ_{KSW}, proposed by Körner, Schierholz and Willrodt [2], is defined for 4-jet events for which there are two jets in both hemispheres defined by the thrust axis. This requirement eliminates about 30% of all 4-jet events. The variable Φ_{KSW} describes the angle between the normal to the plane containing the jets in one hemisphere and the normal to the plane defined by the other two jets. Gluon alignment in the splitting process $g \to gg$ favors $\Phi_{KSW} \approx \pi$, whereas for $g \to q\bar{q}$ the two planes are preferentially orthogonal. Figure 4 shows the corrected nomalized distribution for the variable Φ_{KSW} compared to Monte Carlo predictions for QCD and QCD′ . The differences between QCD and QCD′ are small and the measurements are consistent with either prediction.

The Nachtmann-Reiter angle [3], Θ^*_{NR}, is the angle between the momentum vector differences of jets 1,2 and jets 3,4. On account of the differing helicity structures, $\Theta^*_{NR} \approx 0$ is favored by the process $g \to gg$ ($\frac{d\sigma}{dcos\Theta^*_{NR}} \approx cos^2\ \Theta^*_{NR}$) and $\Theta^*_{NR} \approx \pi/2$ is favored by $g \to q\bar{q}$ ($\frac{d\sigma}{dcos\Theta^*_{NR}} \approx 1 - cos^2\ \Theta^*_{NR}$). Figure 5 shows the measured distribution for $\cos\Theta^*_{NR}$.

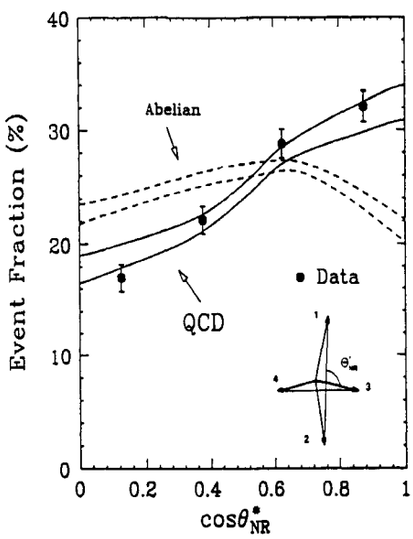

Figure 5: Measured distribution of $\cos\Theta^*_{NR}$. The predictions for QCD and the abelian model QCD′ are shown as bands indicating the theoretical uncertainties.

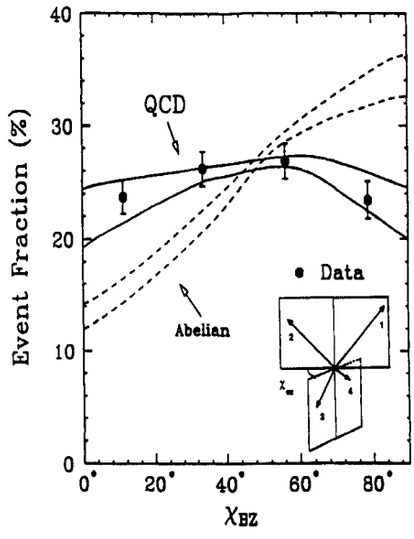

Figure 6: Measured distribution of χ_{BZ} . The predictions for QCD and the abelian model QCD′ are shown as bands indicating the theoretical uncertainties.

The r.m.s. resolution is 6° and the correction due to finite detector resolution and acceptance is less than 7% in the outer two bins and smaller for the central bins. We obtain for three degrees of freedom $\chi^2(QCD) = 5.0$ and $\chi^2(QCD') = 39.8$ for the matrix element predictions, and $\chi^2(QCD) = 0.7$ and $\chi^2(QCD') = 33.2$ for the parton shower approach. In the calculation of the χ^2, a theoretical error due to fragmentation of 2 to 5% per bin is included. The measured distribution in $\cos\Theta^*_{NR}$ clearly favors QCD and is incompatible with the abelian model.

Bengtsson and Zerwas [4] have defined χ_{BZ} as the angle between the plane containing jets 1,2 and the plane containing jets 3,4. Linear polarization of the gluon in $e^+e^- \to q\bar{q}g$ results in different distributions of χ_{BZ} for $g \to gg$ and $g \to q\bar{q}$. The angle χ_{BZ} is distributed nearly isotropically in QCD, while the abelian theory favors $\pi/2$. Figure 6 shows the measured distribution for χ_{BZ}. We have made the requirement that the angle between the jets 1 and 2 and the angle between jets 3 and 4 is less than 160° which reduces the sample of 4-jet events by 40%. The r.m.s. resolution is 6° and the correction due to finite detector reolution and acceptance is at most 10% in the outer two bins and smaller in the center. We obtain for three degrees of freedom $\chi^2(QCD) = 3.0$ and $\chi^2(QCD') = 33.8$ for the matrix element case, and $\chi^2(QCD) = 0.9$ and $\chi^2(QCD') = 61.6$ when using the parton shower evolution. Again we find that the QCD′ model fails to describe our data while QCD reproduces our measurements well.

In addition, we have studied the dependence of the theoretical predictions on the value of y_{cut} in the range 0.02-0.04. QCD can reproduce all measured angular distributions over this range of the jet resolution parameter.

Conclusions

We have studied the angular correlations between jets in 4,200 4-jet events from Z^0 decays. The measured distributions in the angular variables $\cos\Theta^*_{NR}$ and χ_{BZ} are reproduced by QCD, while the predictions of an alternative abelian model are found to be incompatible with our data. The main difference comes from the large rate of $q\bar{q}q\bar{q}$ final states in the abelian model.

Acknowledgements

The author would like to acknowledge her collaborators, particularly T. Hebbeker and S. Schevchenko, for their help in the preparation of this talk.

References

1 M. Gell-Mann, *Acta Physica Austriaca*,Suppl. IX (1072) 733;
H. Fritzsch and M. Gell-Mann, XVI International

Conference on High Energy Physics, Batavia, Vol. II p.135 (172);
H. Fritzsch, M. Gell-Mann and H. Leytwyler, *Phys. Lett.* B 47 (1973) 365.
D.J. Gross and F. Wilczek, *Phys. Rev. Lett.* 30 (1973) 1343;
D.J. Gross and F. Wilczek, *Phys. Rev.* D 8 (1973) 3633;
H.D. Politzer, *Phys. Rev. Lett.* 30 (1973) 1346.

2 J.G. Körner, G. Schierholz and J. Willrodt, *Nucl. Phys.*B 185 (1981) 365.

3 O. Nachtmann and A. Reiter, *Z. Phys.* C 16 (1982) 45.

4 M. Bengtsson and P.M. Zerwas, *Phys. Lett.* B 208 (1988) 306.

5 R.K. Ellis, D.A. Ross and E.A. Terrano, *Nucl. Phys.*B 178 (1981) 421.

6 K.J.F. Gaemers and J.A.M. Vermaseren, *Z. Phys.* C 7 (1980) 81.

7 L3 Collaboration, B. Adeva *et al.*, *Phys. Lett.* B 248 (1990) 462.

8 S. Bethke, A. Ricker and P.M. Zerwas, to be published in *Z. Phys.*

9 L3 Collaboration, B. Adeva *et al.*, *Nucl. Instr. and Meth.*A 289 (1990) 35.

10 T. Sjöstrand, *Comput. Phys. Commun.*39 (1986) 347;
T. Sjöstrand and M. Bengtsson, *Comput. Phys. Commun.*43 (1987) 367;

11 L3 Collaboration, B. Adeva *et al.*, *Phys. Lett.* B 241 (1990) 416.

12 GEANT Version 3.13, September, 1989.
See R. Brun *et al.*, "GEANT 3",
CERN DD/EE/84-1 (Revised), Sept. 1987;

13 L3 Collaboration, B. Adeva *et al.*, *Phys. Lett.* B 237 (1990) 136;
L3 Collaboration, B. Adeva *et al.*, *Phys. Lett.* B 249 (1990) 341;

14 JADE Collaboration, W. Bartel *et al.*, *Z. Phys.* C 33 (1986) 23;
JADE Collaboration, S. Bethke *et al.*, *Phys. Lett.* B 213 (1988) 235.

15 F. Gutbrod, G. Kramer and G. Schierholz, *Z. Phys.* C 21 (1984) 235.

16 Z .Kunszt and P. Nason, in "Z Physics at LEP 1" CERN Report CERN-89-08, Vol.I, p. 373.

DISCUSSION

D. E. Soper *(Univ. Oregon)*: A comment: By a careful analysis, the groups looking at e^+e^- annihilation have demonstrated the existence of the triple-gluon vertex. I would like to point out a connection with one of the talks later in this session, at which results on $p\bar{p} \to$ jets $+x$ will be presented by the CDF group. In $E_T < 50$ GeV or so, most of the jet cross sector would vanish if the triple-gluon vertex were absent. Thus, the comparison of their results to QCD theory will bear most decisively on the question of the nonabelian vertex of QCD.

ARGUS AND CRYSTAL BALL RESULTS ON MESON AND BARYON PRODUCTION IN e^+e^- ANNIHILATION AT $\sqrt{s}$ NEAR $10\,GeV$

U. Volland
Physikalisches Institut, Universität Erlangen-Nürnberg
D-8520 Erlangen, Germany

ABSTRACT

Measurements of inclusive π^0 and η production in non-resonant e^+e^--annihilation events and direct Υ decays are reported from ARGUS and Crystal Ball. An overview of ARGUS results on baryon production in direct Υ decays and $q\bar{q}$-continuum events is given. Measurements from ARGUS of di-proton and di-Λ production are presented and compared with Monte Carlo predictions for the popcorn and diquark production mechanism. The first measurement of inclusive antideuteron production in e^+e^--annihilation is reported by ARGUS and the measured cross section is related to the inclusive production cross section for antiprotons within a simple model.

Introduction

In e^+e^--annihilation the $10\,GeV$ centre-of-mass energy region offers a good possibility to study inclusive hadron production in the continuum process $e^+e^- \rightarrow q\bar{q} \rightarrow$ *hadrons* and in direct Υ decays. While in the continuum process the primary quarks hadronize into the hadrons of the final state, the hadron production in Υ decays is mediated by the fragmentation of gluons. Therefore, a comparison of the inclusive particle yield in continuum processes with that in direct $\Upsilon(1S)$ decays can shed light on possible differences between quark and gluon fragmentation.

New results on meson production from ARGUS and Crystal Ball are reported and measurements of inclusive baryon production from ARGUS are presented. Especially, emphasis is put on recent studies of inclusive baryon production.

Meson Production

ARGUS [1] and Crystal Ball [2] have studied the inclusive π^0 and η production in $e^+e^- \rightarrow q\bar{q} \rightarrow$ *hadrons* events and in direct Υ(1S) decays. The π^0 analyses were performed by reconstructing π^0 mesons from their two-photon decay mode. In each preselected hadronic event the observed photon candidates were grouped into pairs and the invariant mass and the total energy of the two-photon subsystems were calculated. The resulting two-photon invariant mass distribution is analyzed in bins of the scaled energy variable $z = 2\,E_{\gamma\gamma}/\sqrt{s}$, where $E_{\gamma\gamma}$ is total energy of the two-photon system and $\sqrt{s}$ denotes the e^+e^- centre-of-mass energy. For a typical z-bin the mass spectra for continuum data, as obtained by ARGUS and Crystal Ball, are shown in Fig. 1a and 1b, respectively. Prominent π^0 signals with the expected experimental mass resolution are observed.

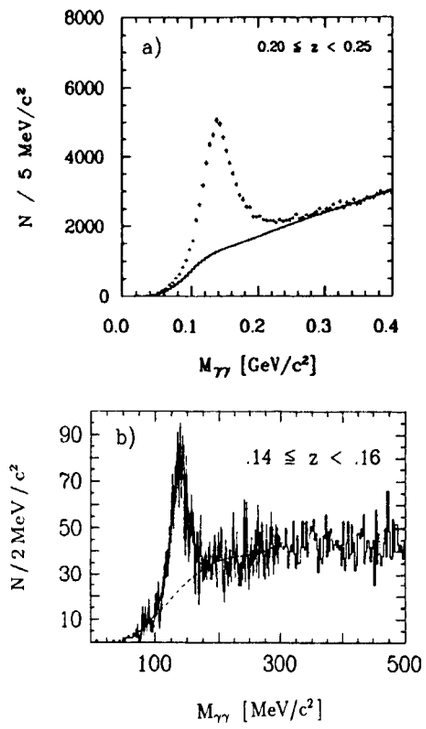

Fig. 1: Two-photon invariant mass distributions for a selected z-bin from a) ARGUS and b) Crystal Ball.

The π^0 yield as a function of z was determined by fitting the spectra with a Gaussian for the π^0 signal on a smooth background, which is either parametrized with a polynominal function (Crystal Ball) or taken from Monte Carlo simulations (ARGUS). For each z-bin, the fitted π^0 yield was corrected for inefficiencies of the π^0 reconstruction algorithm, contributions from τ events, initial state radiation, and for loss of low multiplicity events in the hadronic event selection. The particle spectra are then obtained by dividing the corrected π^0 yield by the number of observed hadronic events and the particle velocity $\beta = pc/E$. The ARGUS spectra together with model predictions for color string and parton shower fragmentation are shown in Fig. 2. For continuum and $\Upsilon(1S)$ data, the measured π^0 spectra are well described by the fragmentation models.

The study of inclusive η production was performed in a rather similar way compared to the π^0 analysis. However, the reconstruction of η mesons from the two-photon decay mode $\eta \to \gamma\gamma$ is hindered by a large combinatorical background due to photons from π^0 decays. This background is reduced by excluding those photons from the η analysis, which are sucessfully paired to combinations reconstructing to the nominal π^0 mass. The η yield is then studied in the invariant mass spectra formed by the remaining two-photon combinations. The η spectra for continuum data and $\Upsilon(1S) \to 3g$ decays, as measured by Crystal Ball, are shown in Fig. 3 together with predictions from different fragmentation models. For continuum data the measured rates are below the model predictions. In direct $\Upsilon(1S) \to 3g$ decays the measured η spectrum differs from the predicted one both in shape and size.

From the measured π^0 and η spectra the mean particle multiplicities per hadronic event were derived by fitting an exponential function to the data and integrating over the whole kinematically allowed z-range. Table 1 summarizes the results on the π^0 and η multiplicities from various experiments performed in the $10\,GeV$ centre-of-mass energy region.

The predictions based on the LUND 6.2/6.3 program [3] for color string [4] and parton shower [5]

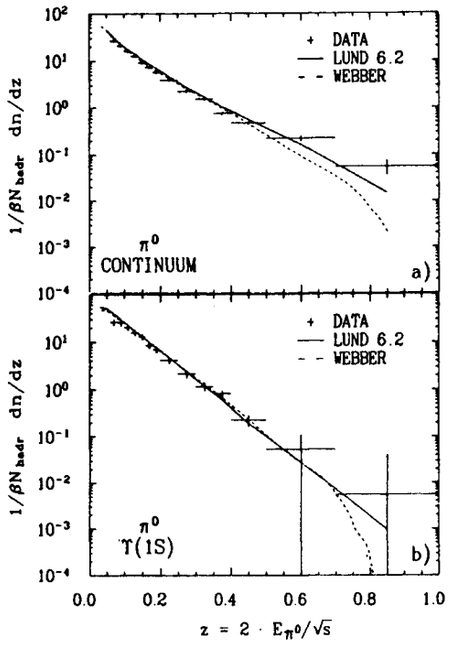

Fig. 2: ARGUS results on the inclusive π^0 spectrum in continuum events and direct $\Upsilon(1S)$ decays. Also shown are Monte Carlo predictions for color string (Lund 6.2) and parton shower (Webber) fragmentation.

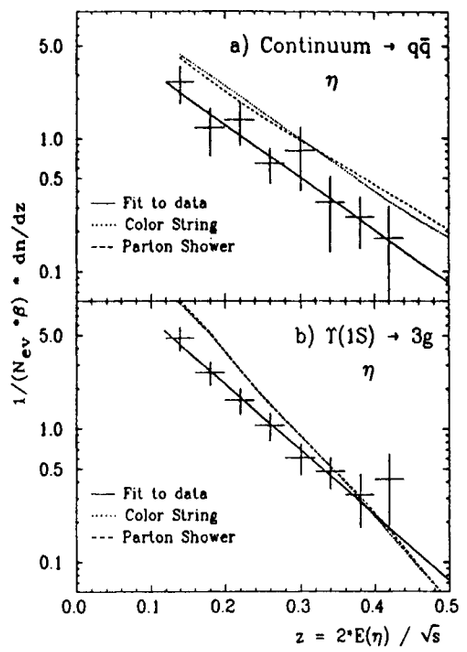

Fig. 3: Crystal Ball results on the inclusive η spectrum in continuum events and direct $\Upsilon(1S)$ decays. Also shown are Monte Carlo predictions for color string and parton shower fragmentation and a fit of an exponential function to the data.

Table 1: Average π^0 and η multiplicties in direct $\Upsilon(1S)$ decays and in $e^+e^- \to q\bar{q} \to$ *hadrons* continuum events as obtained by ARGUS [1], CLEO [6], and Crystal Ball [2]. The LUND 6.2/6.3 model predictions for color string and parton shower fragmentation are listed for comparison.

	$\Upsilon(1S) \to 3g$	Continuum
π^0 Multiplicity		
ARGUS	4.0 ± 0.4	3.2 ± 0.3
CB	3.4 ± 0.4	3.6 ± 0.4
CLEO	5.2 ± 1.8	3.0 ± 0.7
Colour String	4.2	3.6
Parton Shower	4.3	3.5
η Multiplicity		
ARGUS	0.40 ± 0.17	0.19 ± 0.06
CB	0.35 ± 0.06	0.22 ± 0.05
Color String	0.57	0.44
Parton Shower	0.59	0.42

fragmentation are also listed in Table 1. In general the various experiments are in good agreement. The measured π^0 rates are also consistent with the model predictions. The measured η rates are considerably below the model predictions for both the continuum data and direct Υ(1S) decays. This discrepancy may signal some difficulty in the LUND model, where the η rate is tightly bound to the rates of pions and kaons. This discrepancy can only be removed by introducing a further fragmentation parameter in the Lund model.

Baryon Production

While studies of inclusive meson production are useful for model adjustment and comparison, they are rather insensitive to the fragmentation of the primary partons. This is mainly due to the fact that mesons are light particles and are either produced in later stages of the fragmentation cascade or are decay products of heavier resonances.

In this sense a study of inclusive baryon production offers for several reasons interesting features:

- Generally, models differ more widely in the predicted rates for baryons than they do in the meson sector.
- Since baryons are heavy, they are thought to be produced at the early stage of the fragmentation process and can thus yield more direct information on the fragmentation process.
- Flavour dependence, *i.e.* strangeness, of production rates can be studied over a wider range in the baryon sector than in the meson sector.

Δ^{++} *and* $\overline{\Delta^{++}}$ *production*

During the past extensive work [6,7,8] has been done to measure the inclusive production rates of octet and decuplet baryons. The only missing pieces were the Δ-resonances. Their production rates are difficult to measure, since the Δ-baryons are broad resonances and their masses are close to the $p\pi$ threshold. Among the four isospin members of the Δ-resonances, the Δ^{++} offers the best chance for experimental observation. The other isospin partners have either decay modes to final states with neutral particles ($\Delta^+ \to p\pi^0$; $n\pi^+$; $\Delta^- \to n\pi^-$), which are difficult to reconstruct, or considerably smaller branching ratios ($\mathrm{Br}(\Delta^0 \to p\pi^-) = \frac{1}{3} \cdot \mathrm{Br}(\Delta^{++} \to p\pi^+)$).

ARGUS [9] has measured the Δ^{++} and $\overline{\Delta^{++}}$ production rates in Υ(1S) $\to 3g$ decays and in continuum events. Fig. 4 shows the invariant $p\pi^+$ mass spectrum in direct Υ(1S) $\to 3g$ decays after subtraction of the corresponding continuum spectrum, scaled to the same luminosity. The derived production rates in Υ(1S) data and in continuum data are listed in Table 2, together with the measured production rates of other octet and decuplet baryons. The listed rates in Table 2 show the well known trend that baryon production is enhanced in gluon mediated Υ decays by a factor between two and three compared to continuum production.

Flavour suppression can be studied by comparing the production rates for baryons of the same $SU(3)_F$ multiplet, which differ by one unit in strangeness. From the ratios of baryon production rates $< n >_S$ and $< n >_{S'=S-1}$, where S denotes the *strangeness*, one typically obtains values for s-quark over u-quark

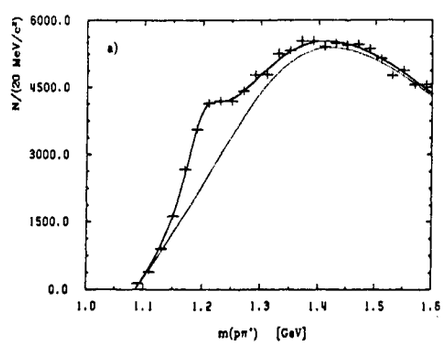

Fig. 4: Invariant mass of $p\pi^+$ combinations from the $\Upsilon(1S)$ resonance. The solid line represents a fit to the data using a smooth four parameter curve and a relativistic Breit-Wigner function, while the dotted line indicates the contribution from background only.

Table 2: ARGUS results [8,9] on baryon production rates for direct $\Upsilon(1S)$ decays and for continuum events. The listed values are the sum of baryon and antibaryon rates. The proton rates are corrected for feeddown from Λ-decays.

Baryon	$\Upsilon(1S) \to 3g$	Continuum
p	0.36 ± 0.03	0.21 ± 0.02
Λ	0.23 ± 0.02	$(0.92 \pm 0.09) \cdot 10^{-1}$
Σ^0	$(5.6 \pm 2.0) \cdot 10^{-2}$	$(2.3 \pm 0.9) \cdot 10^{-2}$
Ξ^-	$(2.1 \pm 0.3) \cdot 10^{-2}$	$(6.7 \pm 0.9) \cdot 10^{-3}$
Δ^{++}	$(1.2 \pm 0.2) \cdot 10^{-1}$	$(4.0 \pm 1.0) \cdot 10^{-2}$
$\Sigma^-(1385)$	$(1.4 \pm 0.3) \cdot 10^{-2}$	$(5.5 \pm 1.5) \cdot 10^{-3}$
$\Sigma^+(1385)$	$(1.7 \pm 0.4) \cdot 10^{-2}$	$(5.1 \pm 1.3) \cdot 10^{-3}$
$\Xi^0(1530)$	$(4.8 \pm 1.3) \cdot 10^{-3}$	$(1.5 \pm 0.6) \cdot 10^{-3}$
Ω^-	$(1.8 \pm 0.7) \cdot 10^{-3}$	$(0.7 \pm 0.4) \cdot 10^{-3}$

suppression of about 0.3, independent of the other two constituent quarks. This value is close to that one found in the meson sector. This is rather unexpected for models, in which baryons are produced via diquarks, since the production of diquarks with strangeness is strongly suppressed compared to single s-quark production. Furthermore, no significant differences are observed between continuum events and $\Upsilon(1S)$ decays.

Spin dependence of baryon production can be studied by forming ratios of rates between the decuplet and octet baryons with the same flavour content. The corresponding ratios for Δ^{++}/p, $\Sigma^{\pm}(1385)/\Sigma^0$ and $\Xi^0(1530)/\Xi^-$, are around 0.3, whereas from naive spin counting one expects a value of $(2 \cdot \frac{3}{2}+1)/(2 \cdot \frac{1}{2}+1) = 2$. Again, no difference is observed in this ratio between quark and gluon fragmentation.

Dibaryon production: pp ($\overline{pp}$) and $\Lambda\Lambda$ ($\overline{\Lambda\Lambda}$)

ARGUS [10] has studied inclusive di-proton and di-Λ production in continuum $e^+e^- \to q\bar{q} \to$ *hadrons* events and in direct $\Upsilon(1S)$ decays. The aim of these studies was to measure the production rates and the angular correlation between the two baryons. Furthermore, the di-baryon rates are expected to be rather sensitive to the production mechanism. Table 3 summarizes the results on inclusive *pp* and $\Lambda\Lambda$ production. Comparing the measured di-proton rates with those for single proton (p and $\bar{p}$) production in the same momentum range shows a suppression by two orders of magnitude. In addition, Monte Carlo predictions based on the LUND model for two different baryon production mechanisms, the popcorn ($\rho = 0.9$) and the diquark ($\rho = 0$) model, are listed in Table 3. The parameter ρ=B M $\overline{\text{B}}$/(B $\overline{\text{B}}$ + B M $\overline{\text{B}}$) describes the flavour correlation in the pair-production of a baryon B and an antibaryon $\overline{\text{B}}$. In the diquark model ($\rho = 0$) the produced baryon and antibaryon carry two common quark flavors, whereas for the popcorn parameter $\rho = 1$ due to the intermediate meson M the B $\overline{\text{B}}$ pair has only one quark flavor in common. From Table 3 it is clear that the popcorn model yields a better description

Table 3: ARGUS results [10] on di-baryon rates for direct $\Upsilon(1S)$ decays and for continuum events. The di-proton rates are measured for particle momenta in the range ($0.4GeV/c < |\vec{p}| < 1.2GeV/c$). The corresponding prediction of the LUND model for the popcorn and diquark production mechanism are also listed.

	$\Upsilon(1S) \to 3\,gluons$	Continuum
$n_{\overline{p}\overline{p}} + n_{pp}$	$(2.0 \pm 0.1) \cdot 10^{-3}$	$(4.5 \pm 0.5) \cdot 10^{-4}$
Popcorn	$1.0 \cdot 10^{-2}$	$5.6 \cdot 10^{-4}$
Diquark	$1.6 \cdot 10^{-2}$	$1.9 \cdot 10^{-3}$
$n_{\overline{\Lambda}\overline{\Lambda}} + n_{\Lambda\Lambda}$	$(1.8 \pm 0.5) \cdot 10^{-3}$	$(5.1 \pm 3.7) \cdot 10^{-4}$
Popcorn	$1.7 \cdot 10^{-3}$	$1.8 \cdot 10^{-4}$
Diquark	$5.3 \cdot 10^{-3}$	$1.2 \cdot 10^{-3}$

of the data than the diquark model. However, the predicted pp rates in direct Υ decays are still a factor five too large.

ARGUS has also analyzed the angular correlation between two protons or two antiprotons produced in continuum events and direct Υ decays [10]. The resulting distributions of the opening angle ϑ_{pp} are displayed in Fig. 5 together with absolute Monte Carlo predictions for the popcorn option of the Lund model. Whereas for continuum data a qualitative agreement between data and model prediction is achieved, the predicted distribution in direct Υ decays deviates considerably both in magnitude and shape from the measured one.

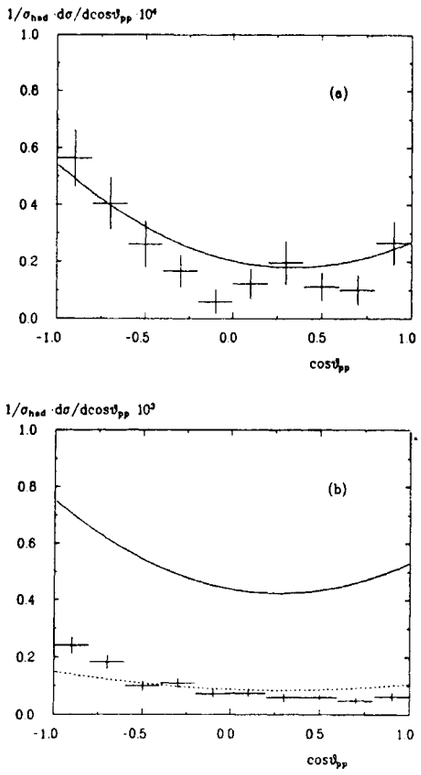

Fig. 5: Distribution of the opening angle between two protons (antiprotons) for a) continuum data and b) direct Υ decays. The solid lines represent the predictions of the Lund model with a popcorn fraction of 0.9. The dashed line in Fig. 5b corresponds to the Lund prediction normalized to the experimental data.

Antideuteron $\bar{d}$ production in direct Υ decays

ARGUS has observed antideuteron production in direct $\Upsilon(1S,2S)$ decays [11]. The analysis is based on $\Upsilon(1S)$ and $\Upsilon(2S)$ data of together $70pb^{-1}$ and a combined continuum sample consisting of $47pb^{-1}$ continuum events and $105pb^{-1}$ of data taken at the $\Upsilon(4S)$ resonance. Antideuteron candidates are well identified from dE/dx and time-of-flight measurements for particle momenta below $1.7\,GeV/c$.

We find 19 hadronic events with an antideuteron candidate in the $\Upsilon(1S,2S)$ data sample and two events in the combined continuum data sample. For the latter two events the kinematics of the $\bar{d}$ candidates were incompatible with originating from B-decays, but are consistent with the estimated fake rate from overlapping tracks and particle misidentification. Scaling this background to the size of the $\Upsilon(1S,2S)$ data sample results in only one background event. Therefore, we attribute the 19 events observed in the $\Upsilon(1S,2S)$ data to direct Υ decays.

After correcting for background and acceptance we derive from the 19 observed events the momentum spectrum of $\bar{d}$ production in direct $\Upsilon(1S,2S)$ decays. The resulting spectrum is shown in Fig. 6, together with a fit to the data of a phenomenological function to describe the shape of the momentum distribution. Extrapolating the fit result into the unmeasured momentum region, we derive an $\bar{d}$

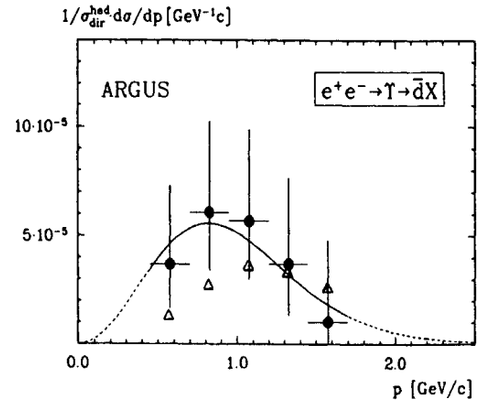

Fig. 6: The momentum dependence of the cross section for inclusive antideuteron production in direct hadronic $\Upsilon(1S,2S)$ decays. The solid line represents a fit of a phenomenological function to the data. Open triangles indicate the $\bar{d}$ cross section as calculated within a simple model using as input the measured cross section for $\bar{p}$ production.

production rate of $(6.0 \pm 2.0 \pm 0.6) \cdot 10^{-5}$ per direct $\Upsilon(1S, 2S)$ resonance decay. This rate is four orders of magnitude smaller than the measured rate for inclusive $\bar{p}$ production. In addition, from the two events in the continuum sample we derive an upper limit (90% CL) of $1.7 \cdot 10^{-5}$ on $\bar{d}$ production in $q\bar{q}$-events.

Taking a simple model [12], used in high energy nucleus-nucleus collisions to explain deuteron production, we relate the measured $\bar{d}$ cross section to the $\bar{p}$ cross section. With the basic assumptions that $\bar{p}$ and $\bar{n}$ are produced uncorrelated and with equal cross sections and that $\bar{p}$ and $\bar{n}$ coalesce into an $\bar{d}$ if they are close enough in phase space, the inclusive $\bar{d}$ cross section can be written in a factorized form:

$$\frac{1}{\sigma_{dir}^{had}} \cdot \frac{\mathrm{d}^3\sigma(\bar{d})}{\mathrm{d}^3\mathrm{p}} = \frac{4\pi}{3} \mathrm{p}_0^3 \gamma \cdot \left(\frac{1}{\sigma_{dir}^{had}} \frac{\mathrm{d}^3\sigma(\bar{p})}{\mathrm{d}^3\mathrm{p}}\right) \cdot \left(\frac{1}{\sigma_{dir}^{had}} \frac{\mathrm{d}^3\sigma(\bar{n})}{\mathrm{d}^3\mathrm{p}}\right)$$

The first term on the right hand side describes the coalescence volume and is characterized by p_0, the Fourier transform of the spatial size of the $\bar{d}$ wave function. With $\mathrm{p}_0 = 130 MeV/c$, taken from Ref. [13], and the known inclusive $\bar{p}$ cross section we can calculate the inclusive $\bar{d}$ cross section within this model. The open triangles in Fig. 6 indicate the result of this model calculation. Having in mind that the model neither accounts for the limited phase space nor is fully relativistic, it is surprising that such a simple model reproduces the observed suppression by four orders of magnitude correctly. Certainly for describing fine details of the $\bar{d}$ momentum spectrum the model is too simple and the available statistics too small.

Conclusions

New results on inclusive π^0 and η production were obtained by ARGUS and Crystal Ball. These measurements are valuable for comparison with fragmentation models and adjustment of model parameters.

ARGUS has measured in e^+e^--annihilation at $\sqrt{s} \approx 10 GeV$ the production rates of all octet and decuplet baryons. These rates allow to study the spin and flavor dependence of quark and gluon fragmentation. Sensitive tests of the underlying physics basis of fragmentation models are obtained from ARGUS measurements of inclusive pp $(\bar{p}\,\bar{p})$ and $\Lambda\Lambda$ $(\bar{\Lambda}\,\bar{\Lambda})$ production and from the study of angular correlations. For the first time the production cross section of a composed baryon, the antideuteron $\bar{d}$, is measured in e^+e^--annihilation. The observed rate can be reproduced from the $\bar{p}$ production cross section within a simple coalescence model.

Acknowledgement: This work was supported in part by the BMFT under contract No. 054ER12P.

References

[1] H. Albrecht *et al.* (ARGUS), *Z. Phys.* **C46** (1990) 15.

[2] Ch. Bieler *et al.* (Crystal Ball), DESY 90-086, to be published in *Z. Phys. C.*

[3] T. Sjöstrand, *Comp. Phys. Comm.* **39** (1986) 347; T. Sjöstrand and M. Bengtsson, *Comp. Phys. Comm.* **43** (1987) 367.

[4] B. Andersson *et al.*, *Phys. Rep.* **97** (1987) 31.

[5] G. Marchesini and W. R. Webber, *Nucl. Phys.* **B238** (1984) 1; W. R. Webber, *Nucl. Phys.* **B238** (1984) 492.

[6] S. Behrends *et al.* (CLEO), *Phys. Rev.* **D31** (1985) 2161.

[7] M.S. Alam *et al.* (CLEO), *Phys. Rev. Lett.* **53** (1985) 24;

[8] H. Albrecht *et al.* (ARGUS), *Z. Phys.* **C44** (1989) 547; *Z. Phys.* **C43** (1989) 45; *Z. Phys.* **C39** (1988) 177; *Phys. Lett.* **B183** (1987) 419;

[9] H. Albrecht *et al.* (ARGUS), *Phys. Lett.* **B230** (1989) 169.

[10] H. Albrecht *et al.* (ARGUS), DESY 90-33.

[11] H. Albrecht *et al.* (ARGUS), *Phys. Lett.* **B236** (1990) 102.

[12] H. H. Gutbrod *et al.*, *Phys. Rev. Lett.* **37** (1976) 667; H. Sato and K. Yazaki, *Phys. Lett.* **B98** (1981) 153.

[13] J. Gosset *et al.*, *Phys. Rev.* **C16** (1977) 629; M. C. Lemaire *et al.*, *Phys. Lett.* **B85** (1979) 38; V. B. Gavrilov *et al.*, *Z. Phys.* **A324** (1986) 75.

DISCUSSION

C. Buchanan *(UCLA)*: I would like to comment that the UCLA hadronization modeling, which is a spin-off of the Lund model and uses the Lund Symmetric Fragmentation Function as a production density controlling heavy particle production does rather well on some of your interesting data: our n prediction is lower than Lund's; we predict your Λ and pp rate rather naturally. I would like to compare our predictions with your updated strange baryon rates.

COMPARISON OF QUARK AND GLUON JETS USING THREE-JET EVENTS FROM e^+e^- ANNIHILATION AT TRISTAN

MINGHAN YE

National Laboratory for High Energy Physics,Tsukuba, Ibaraki, 305 JAPAN

and

Institute of High Energy Physics, Beijing 100039, China

Representing the AMY Collaboration

ABSTRACT

Three-jet events produced in e^+e^- annihilations are used to demonstrate differences between quark-induced and gluon-induced jets. Quark jets tend to have a more tightly collimated structure than gluon jets, which is reflected in a higher concentration of the jet's energy near the jet axis, a higher rapidity relative to the jet direction of the most energetic particle in a jet, and a narrower distribution of the Energy-Energy Correlation.

High-energy e^+e^- annihilations into $q\bar{q}g$ final states, which appear in the laboratory as $e^+e^- \rightarrow$ three jets of hadrons, have a simple underlying parton structure that makes them well-suited for comparisons of the hadronization process for quarks and gluons. In this paper, we report on a comparison of various properties of samples of quark-enriched and gluon-enriched jets extracted from $e^+e^- \rightarrow$ three-jet events observed in the AMY detector at center-of-mass energies between $\sqrt{s} =$ 50 GeV and 60.8 GeV. Parts of this work has been reported earlier [1].

Since the discovery of $e^+e^- \rightarrow$ three-jet events, they have been used for many experimental searches for differences between quark jets and gluon jets. The Mark-II collaboration at the PEP storage ring studied the inclusive momentum spectrum of particles and reported a softer fragmentation for gluon jets [2]. This analysis involved extrapolating data from other experiments for quark jets, with the possibility that there may be large systematic errors. A similar study has been done by the TASSO collaboration at the PETRA storage ring using three-jet events at $30 < \sqrt{s} < 38$ GeV and two-jet events at $22 < \sqrt{s} < 25$ GeV [3]. They reported no evidence for any differences, in contradiction with the MARK-II results, and suggested an explanation of the Mark II results in terms of the selection cuts applied to the different jet samples. The JADE group at PETRA reported a higher average value of transverse momentum relative to the jet axis, $< p_t >$, for gluon jets [4]. Averaging over jet energies between 6 and 10 GeV, they found $< p_t >_3 / < p_t >_2 = 1.16 \pm 0.02$, indicating wider gluon jets. Preliminary results from the TPC group at PEP showed that gluon jets appear to be fatter than quark jets in the average transverse momentum in the event plane, $< p_t^{in} >$; they found $< p_t^{in} >_3 / < p_t^{in} >_2 = 1.08 \pm 0.02$ [5]. The CELLO group at PETRA compared the lowest energy jet in three-jet events at 35 GeV center-of-mass energy with a quark jet at 14 GeV center-of-mass energy. They reported preliminary results that show no evidence for any differences, namely $< p_t >_3 / < p_t >_2 = 1.03 \pm 0.05$, in contradiction to the JADE results [6]. The HRS group at PEP [7] looked at the charged multiplicities, n_{chg}, of quark and gluon jets using "nearly-symmetric" three-jet events and compared the results with a Monte Carlo (MC) model. Within experimental errors, no strong differences were observed; $< n_{chg} >_g / < n_{chg} >_q = 1.29^{+0.21}_{-0.41} \pm 0.20$.

The AMY detector and the procedure for selecting multihadron events are described in ref. [8]. Jets are formed by means of the jet-clustering al-

gorithm developed by the JADE group [9] using a cutoff parameter value of $y_{cut} = (9\text{GeV})^2/s$.

We apply the following additional selection criteria to those events that contain three jets. An event is rejected if any of the three jets contains less than four particles, or has a visible energy $E^{jet}_{vis} \leq 6$ GeV, or has $|\cos\theta_{jet}| \geq 0.7$. To select planar events, we require the sum of jet-jet opening angles to be $\geq 358°$. To eliminate events where one of the jets is erroneously formed by clustering a hard photon from initial-state radiation with some random low-momentum particles, we reject events if any jet contains a neutral particle with energy $\geq 0.8E^{jet}_{vis}$. From the original sample of 3230 multihadron events, 336 events pass the selection criteria.

We determine the "calculated" energy of each jet, E^{jet}_{cal}, using energy-momentum conservation and the opening angles between the three jets. Here we neglect the jet's invariant mass. We categorize the jets in each event according to their calculated energy values; jet-1 and jet-2 (the quark-enriched jets) are the highest energy jets and jet-3 (the gluon-enriched jet), the lowest energy jet. To eliminate jets that have many missing or mismeasured particles, we require $\frac{2}{3} \leq (E^{jet}_{vis}/E^{jet}_{cal}) \leq \frac{4}{3}$. This cut, which is applied to individual jets and not to the entire event, eliminates 25% of the jets.

Since the gluon-enriched jet sample corresponds to the jets with the lowest value of E^{jet}_{cal} in each event, there is little energy overlap with jets in the quark-enriched sample over our range of center-of-mass energies. Thus, comparisons are best done using variables that have little variation with E^{jet}_{cal}. It has been shown that quarks and gluons do not hadronize independently in an event [10], which introduces ambiguities into the the assignment of particles to jets. These, however, affect mainly the soft particles; the high momentum particles are produced nearly independently of inter-parton correlations [11]. In order to reduce the uncertainties due to soft particles, we prefer to rely on variables that are dominated by high momentum particles instead of variables that are uniformly weighted by all particles, such as n_{chg} and $< p_t >$. Specifically, we define the variables:

- **the core-energy fraction, ξ ;**

  the fraction of E^{jet}_{vis} that is contained in a cone of half angle $\theta_{cone} = 60°/\sqrt{E^{jet}_{cal}}$ that is coaxial with the jet direction.

- **the rapidity of the leading particle, η ;**

  the rapidity of the leading particle in a jet, relative to the jet axis.

- **the integrated Energy-Energy Correlation, Σ^{30} ;**

  the Energy-Energy Correlation EEC is the pairwise distribution of opening angles of each pair of particles in the jet weighed by their fractional energies. We define the integrated EEC as the integral of the normalized EEC between 0° and 30°;

  $$\Sigma^{30} = \int_0^{30°} \frac{d\Sigma}{d\theta} d\theta.$$

  Note that the normalization is such that $\Sigma^{180} = 1$.

Since ξ is determined by the energy flow in the core of a jet, η is determined from the most energetic particle in a jet, and Σ^{30} is an energy weighted variable, all of these variables are dominated by high momentum particles in different ways.

Since we are trying to compare properties of quarks and gluons, which are unobservable, we are forced to rely on theoretical models for guidance. Two different QCD-motivated Monte Carlo event generators are used: the Lund 6.2 Matrix Element model [12] with the independent fragmentation scheme of Hoyer et al. [13], subsequently called the $q = g$ model, and the Lund 6.3 Parton Shower model with the string fragmentation [12], subsequently called the PS model. In both cases, samples of generated events are passed through the detector simulation program and are subjected to the

same three-jet analysis that is used for the data. In the $q = g$ model, the same algorithm is used to hadronize quarks and gluons and, thus, we don't expect any differences between the resulting jets. These events are used as a "control sample" to verify that the detector acceptance and our analysis procedures are not introducing artificial differences between quark and gluon jets.

In addition to the above-noted variables, we have also examined the more commonly used variables $< p_t >$ and n_{chg}, which are determined using all particles and charged particles, respectively, without any momentum weighting. Figures 1 and 2 show the mean values of $< p_t >$ and n_{chg} as a function of E^{jet}_{cal}, respectively. The jet-3 sample appears to favor higher $< p_t >$, i.e. wider jets and higher n_{chg}, i.e. softer hadronization at the same jet energies, although these differences are not very dramatic.

In Fig. 3 we show the mean value of the core-energy fraction ξ as a function of E^{jet}_{cal} for the jet-1,2 and jet-3 samples. This variable is not too sensitive to the jet energy. The data indicate that in quark jets the energy is concentrated near the jet axis, while in gluon jets it tends to be diffuse. The results for the $q = g$ MC event sample for the jet-1,2 and jet-3 samples, shown in the figure as solid

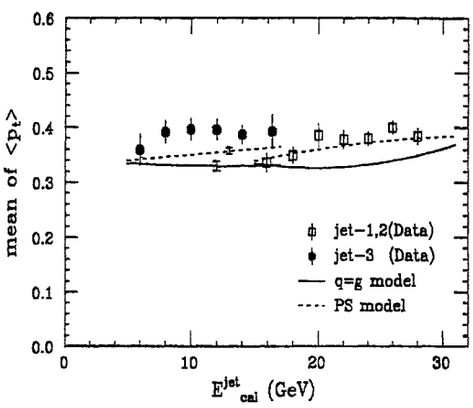

Figure 1: The mean values of the average transverse momentum $< p_t >$ as a function of E^{jet}_{cal} for all neutral and charged particles. The solid (open) points are for the gluon-enriched (quark-enriched) jet sample. The solid (dashed) lines are the expectations from the ME + $q = g$ model (PS + string fragmentation model).

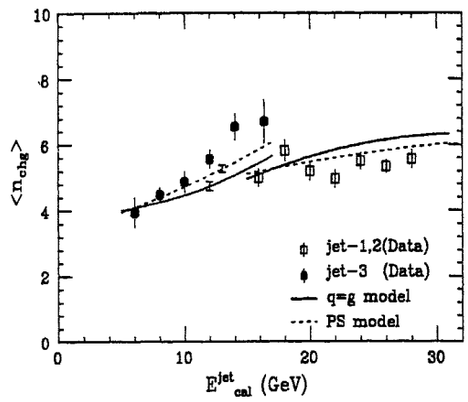

Figure 2: The mean values of the charged-particle multiplicity $< n_{chg} >$ as a function of E^{jet}_{cal}.

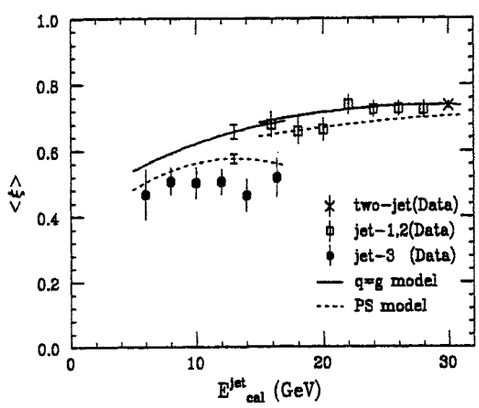

Figure 3: The mean core-energy fraction, ξ, as a function of the calculated jet energy, E^{vis}_{cal}. The cross indicates the result from the two-jet events.

lines, shows no significant discontinuity between the different jet samples; it agrees reasonably well with the jet-1,2 data points and lies considerably above those from the jet-3 sample.

Figure 4 shows the mean values of the leading particle's rapidity, η, which also indicate some distinction between the different jet samples. The leading particles tend to have a higher rapidity in quark jets than in gluon jets. Here, the results of the $q = g$ MC lie somewhat higher than the jet-1,2 data points but substantially overestimate those from jet-3.

The normalized EEC distribution is shown in Fig. 5 for the lowest energy portion of the jet-1,2 sample ($E^{jet}_{cal} \leq 19$ GeV; average=17.0 GeV)

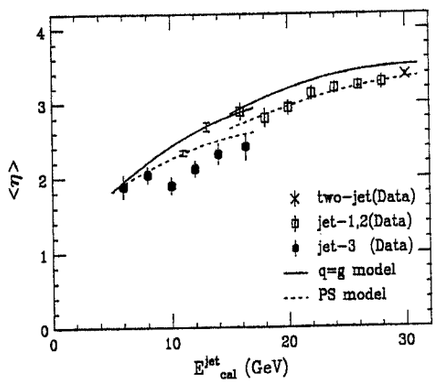

Figure 4: The mean rapidity of the leading particle in the jet, η, as a function of the calculated jet energy, E^{jet}_{cal}.

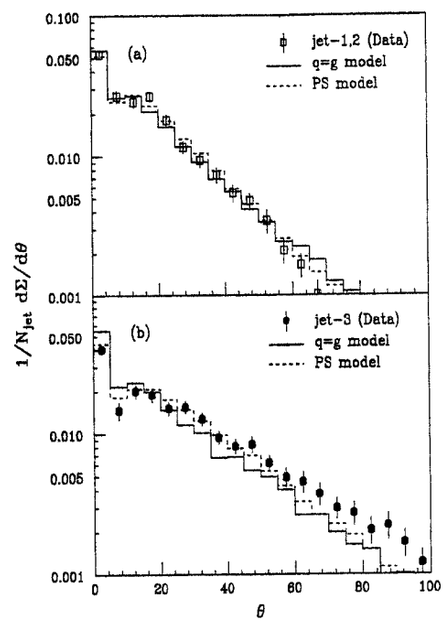

Figure 5: The normalized Energy-Energy Correlation, $d\Sigma/d\theta$, for the (a) quark-enriched jets with $E^{jet}_{cal} < 19$ GeV and (b) gluon-enriched jets with $E^{jet}_{cal} > 13$ GeV. All distributions are normalized to have unit integral.

and the highest energy portion of the jet-3 sample ($E^{jet}_{cal} \geq 13$ GeV; average=14.7 GeV), respectively. The peak in the first bin is the particles' self correlation (i.e., when $i = j$). The $q = g$ MC event sample gives reasonable agreement with our data for jet-1,2 sample while the jet-3 distribution for the data sample is wider than that of $q = g$ MC sample. Figure 6 shows the mean values of Σ^{30}, the integral of the EEC distribution between 0° and 30°, as a function of E^{jet}_{cal}, for the jet-1,2 and jet-3 samples. This also indicates some distinctions between the different jet samples.

The predictions of the PS model are shown as dashed lines in Figs. 1, 2, 3, 4, 5, and 6. The agreement with the jet-1,2 data sample is reasonably good and the model's different treatment of quarks and gluons results in a different predicted behavior for the jet-3 sample. This difference, while evident in all four figures, is not as strong as the differences observed in the data.

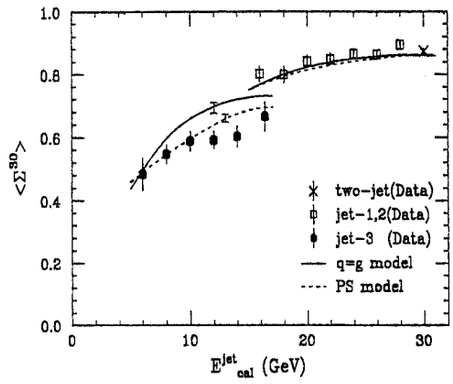

Figure 6: The mean of Σ^{30} as a function of the calculated jet energy, E^{jet}_{cal}.

In Figs.7 (a) and (b), we show distributions in ξ for the lowest energy portion of the jet-1,2 sample ($E^{jet}_{cal} \leq 19$ GeV; average=17.0 GeV) and the highest energy portion of the jet-3 sample ($E^{jet}_{cal} \geq 13$ GeV; average=14.7 GeV), respectively. The distributions for the jet-1,2 and jet-3 samples show a strikingly different character. The quark-enriched sample peaks at $\xi = 1$, corresponding to 100% of the visible energy in the core, while the gluon-enriched sample favors smaller values of ξ, corresponding to little of the visible energy in the core. The solid-line histograms are the results from the $q = g$ MC events. These give very similar distributions in both cases, showing reasonable agreement with the quark-enriched data sample ($\chi^2 = 11.9$ for 9 degrees of freedom) and clear disagreement

with the gluon-enriched data sample ($\chi^2 = 49.6$). The PS model (dashed lines) predicts some distinction between the different jet samples although not as much as is observed in the data. The PS model gives good agreement with the jet-1,2 sample ($\chi^2 = 3.9$); the agreement with the jet-3 data is worse ($\chi^2 = 19.4$).

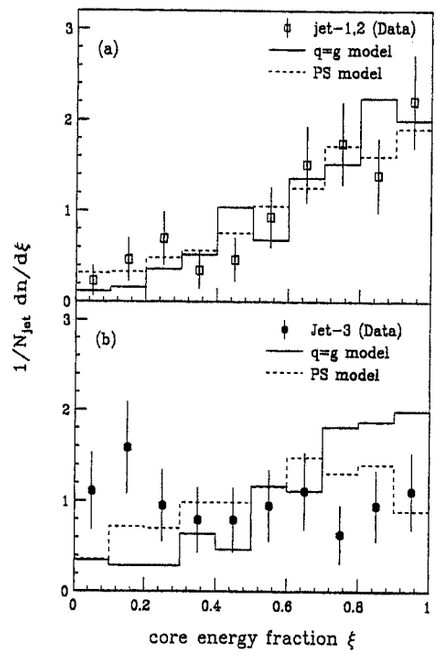

Figure 7: The core-energy fraction distributions (ξ) for the (a) quark-enriched jets with $E_{cal}^{jet} < 19$ GeV and (b) gluon-enriched jets with $E_{cal}^{jet} > 13$ GeV.

To check for possible systematic sources for the observed differences between the jet-1,2 and jet-3 samples, we made the comparison for a variety of selection criteria. The differences reported here are not very sensitive to our choice of selection criteria [11].

References

[1] Y.K. Kim (AMY Collaboration), Phys. Rev. Lett. **63**, 1772 (1989).

[2] A. Petersen *et al.* (Mark II Collaboration), Phys. Rev. Lett. **55**, 1954 (1985).

[3] W. Braunschweig *et al.* (TASSO Collaboration), Z. Phys. **C45**, 1 (1989).

[4] W. Bartel *et al.* (JADE Collaboration), Phys. Lett. **123B**, 460 (1983).

[5] R.J. Madaras *et al.* (TPC Collaboration), Rencontre de Moriond on Strong Interactions and Gauge Theories, Les Arcs (1986).

[6] Cello Collaboration, contributed paper at the International Symp. on Lepton and Photon Interactions at High Energies, Hamburg (1987).

[7] M. Derrick *et al.* (HRS Collaboration), Phys. Lett. **165B**, 449 (1985); K. Sugano, Int. J. Mod. Phys. **A3**, 2249 (1988).

[8] T. Kumita *et al.* (AMY Collaboration) KEK preprint 89-188, submitted to Physical Review D.

[9] S. Bethke, LBL-25247, March 1988. Presented at XXII Rencontre de Moriond, March 1988.

[10] W. Bartel *et al.* (Jade Collaboration), Z. Phys. **C21** (1983); Phys. Lett. **134B**, 275 (1984); **157B**, 340 (1985); M. Aihara *et al.* (TPC Collaboration), Z. Phys. **C28**, 31 (1985); M. Althoff *et al.* (TASSO Collaboration), Z. Phys. **C29**, 29 (1985).

[11] Y.K. Kim (AMY Collaboration), Ph.D. Thesis, University of Rochester (1990), unpublished.

[12] M. Bengtsson, T. Sjöstrand, Phys. Lett. **185B**, 435 (1987). M. Bengtsson, T. Sjöstrand, Nucl. Phys. **B289**, 810 (1987).

[13] P. Hoyer, P. Osland, H.G. Sander, T.F. Walsh, P.M. Zerwas, Nucl. Phys. **B161**, 349 (1979).

DISCUSSION

Q. **R. Blair** *(ANL)*: Are there plans to run at lower $\sqrt{s}$ to provide quark jet data that better overlaps the gluon jet data?

A. **M. H. Ye**: The data are limited by the energy range of the accelerator. There is an overlap, but it is only over a narrow range of jet energies.

JET STUDIES IN CDF

The CDF Collaboration
(The collaborating institutions are listed in the Appendix)

Presented by Mauro Dell'Orso
Dipartimento di Fisica, Università di Pisa
Pisa, Italy

ABSTRACT

Measurements are presented of inclusive jet, two-jet, and three-jet productions at the Fermilab Tevatron Collider at $\sqrt{s}$ = 1.8 TeV. These measurements contain jets up to 400 GeV in transverse energy and dijet masses up to 950 GeV. Comparisons have been made to perturbative QCD predictions at both orders α_s^2 and α_s^3.

INTRODUCTION

Data taken in 1988 and 1989 at the Fermilab collider have resulted in significant advances in the study of high energy proton-antiproton collisions. The current CDF data sample, collected at $\sqrt{s}$ = 1800 GeV, corresponds to approximately 4.5 pb^{-1} of integrated luminosity. This paper presents preliminary measurements of (i) inclusive jet production, (ii) two-jet production, and (iii) three-jet production.

The interest for such measurements at the highest jet energies is manifold.

a) Comparisons to perturbative QCD can be made over a large range of jet energies.
b) The point-like scattering of partons can be probed at distances smaller than 5×10^{-17} cm [1].
c) The dependence of the cross section on the jet clustering cone size, featured by the α_s^3 QCD predictions now available [2], can be studied.
d) New and unexpected physics can show up as resonance bumps or, for negative results, limits can be defined on the mass and coupling to partons of such new particles.

DATA SELECTION

The CDF detector has been described in detail elsewhere [3]. For these measurements jets in the central scintillator calorimeter and in the endplug gas calorimeter were used. For the inclusive jet and for the dijet analysis, the data were collected using single jet online triggers. These triggers basically required the presence of at least one energy cluster in the calorimeter with a transverse energy greater than, respectively, 20, 40, and 60 GeV. The 20 and 40 GeV jet triggers were pre-scaled. The data for the three-jet analysis were collected with a total E_t trigger requiring a total transverse energy in the calorimeter greater than 120 GeV.

Offline jets are clustered with a fixed cone size algorithm [4]. The cone size is defined by $R = (\Delta\eta^2 + \Delta\varphi^2)^{1/2}$, where η and φ represent the pseudorapidity and the azimuthal angle. The algorithm also gives the momentum of each jet, assuming a massless particle for each calorimeter tower belonging to the cluster.

DETECTOR RESPONSE

The effects of resolution smearing and energy degradation due to calorimeter non-linearities, uninstrumented regions of detector, etc. can distort the measured spectra. In order to take into account these effects, a Montecarlo was used [5]. It was tuned to reproduce the calorimeter response to single pions observed in the test beam and the jet fragmentation observed in the data. The E_t and the M_{jj} (dijet mass) response functions were then extracted. These informations were used when comparing the data to the theoretical predictions.

The major sources of systematic error on the jet energy scale result from uncertainties on the calorimeter

response and on the fragmentation tuning in the Montecarlo. The preliminary estimate of the overall systematic error in the jet energy scale varies from 4% at 20 GeV to 3% at 400 GeV, however the correlations between the systematic errors at different jet energies are still under study. After including the reflection of the error on the energy scale and a 15% systematic uncertainty on the integrated luminosity, the systematic error on the cross section ranges from 23% to 60% depending on the jet E_t.

It should be noted that, when comparing the data to the theory, there is a theoretical uncertainty in the definition of underlying event and of out-of-cone energy that cannot be neglected.

INCLUSIVE JET PRODUCTION

For this measurement jets in the central pseudorapidity region ($0.1 < |\eta| < 0.7$) were selected. Fig. 1 shows the differential cross section as a function of E_t for a cone size of 0.7 compared to a leading order QCD calculation (solid line).

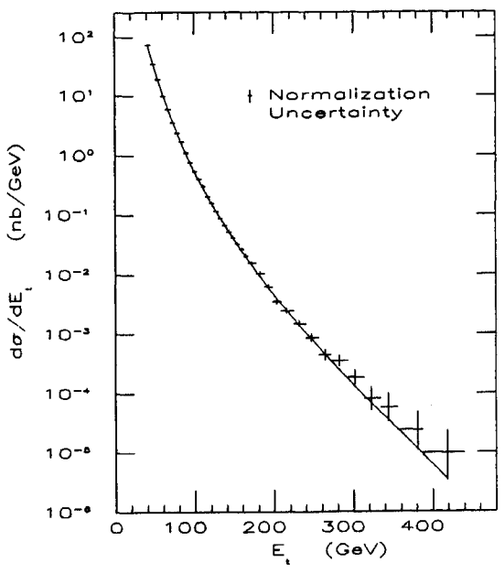

Fig. 1 Inclusive jet cross section compared to leading order QCD (CDF preliminary).

The data were corrected using the detector response, the underlying event energy was subtracted, and no out-of-cone correction was applied. The error bars on the data points represent the statistical errors only. The QCD prediction shown in fig. 1 uses the structure functions EHLQ1 [2] and $Q^2 = 0.5\ P_t^2$. This prediction was normalized to the data by fitting a global normalization factor in the low E_t region ($E_t < 164$ GeV).

Since QCD and compositeness will agree in shape in the low E_t region and disagree at high E_t, in order to search for compositeness the data must be compared to the predictions in the high E_t region. A slight excess of events can be seen in this region in fig. 1. The statistical level of this excess, however, is only 2.5 to 3.5 standard deviations (depending on the structure function) and it will be reduced some more when the systematic error will be taken into account.

Fig. 2 shows the same data now compared to next-to-leading order QCD, where the QCD normalization is absolute. The comparison on absolute scale is interesting here, since the next-to-leading order prediction has a reduced theoretical uncertainty. The QCD calculation uses the structure functions MRSB [6] and $Q^2 = 0.25 P_t^2$.

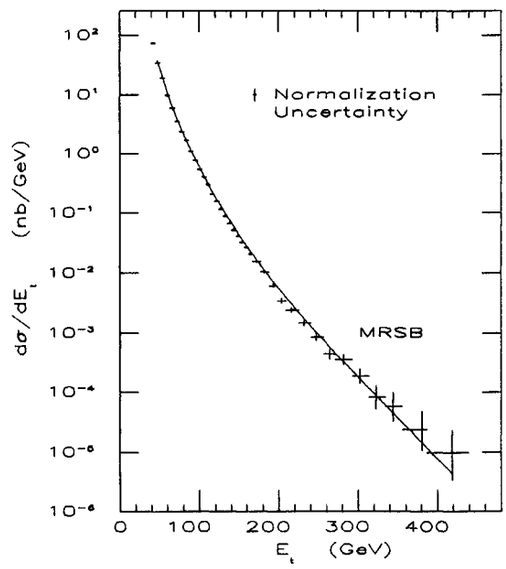

Fig. 2 Inclusive jet cross section compared to next-to-leading order QCD (CDF preliminary).

A comparison is also made to next-to-leading order QCD in fig. 3. The top plot in this figure shows the cross section as a function of cone size for 100 GeV E_t jets. The error bars on the data points represent the statistical errors. The data appear to be consistent with QCD within the systematic uncertainty on the vertical

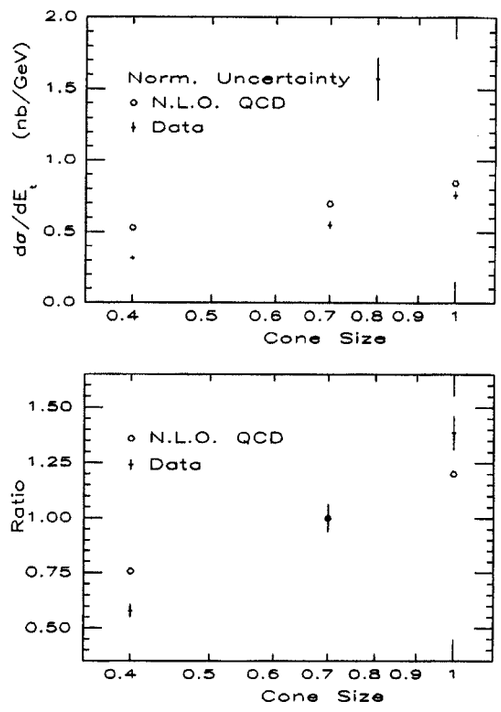

Fig. 3 Cross section at E_t = 100 GeV as a function of the clustering cone size (CDF preliminary).

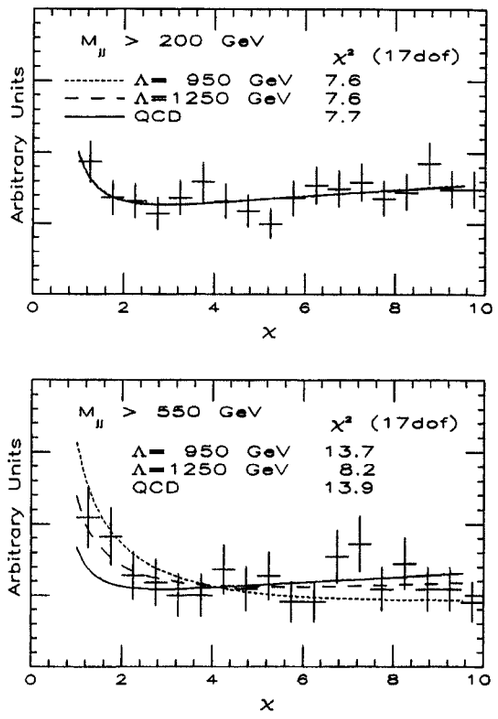

Fig. 4 Distribution of $\chi = (1+\cos\theta)/(1-\cos\theta)$ for dijet events (CDF preliminary).

scale. To get rid of most of the systematic uncertainty we can compare the slope of the data to the slope of the prediction. To this purpose the bottom plot in fig. 3 shows the computed and the measured cross sections for different cone sizes, respectively normalized to the computed and the measured cross sections for a cone size of 0.7. In this plot the data appear to have a steeper dependence on the cone size than what α_s^3 calculations would predict.

DIJET PRODUCTION

Additional tests of QCD involve the study of dijet events; we measured the dijet angular distribution and the dijet invariant mass spectrum. The two leading jets in an event are used to define the dijet system. In the center of mass frame, the two jets are back to back and they are described by the dijet invariant mass M_{jj} and by the scattering angle θ (the angle between the jets and the incoming beam). Fig. 4 shows the distribution of $\chi = (1+\cos\theta)/(1-\cos\theta)$ for two ranges of invariant masses, namely $M_{jj} > 200$ GeV and $M_{jj} > 550$ GeV. The same plots show the theoretical predictions for leading order QCD and for different compositeness scales. The calculation uses the structure functions DO1 [7]. The effect of composite quarks is approximated by an effective four-fermion contact interaction [2]. The normalization of the theory curves is chosen to minimize the chi-square.

The dijet invariant mass was calculated as $M_{jj} = [(E_1+E_2)^2-(\mathbf{P}_1+\mathbf{P}_2)^2]^{1/2}$, where E_i and $\mathbf{P}_i$ are the measured energies and momenta of the two leading jets. Since the next to leading order QCD predictions are available only for the inclusive jet production, for the measurement of the differential cross section as a function of M_{jj} an out of cone correction has been applied to the jet energies. Moreover, instead of correcting the data for the finite resolution, the theoretical predictions were smeared using the M_{jj} detector response [8]. This procedure simplifies the search for bumps, since correcting the data would require in input the data line shape.

Fig. 5 shows the measured differential cross section $d\sigma/dM_{jj}$, integrated over the pseudorapidity range $|\eta| < 0.7$, as a function of M_{jj}. The dots represent the

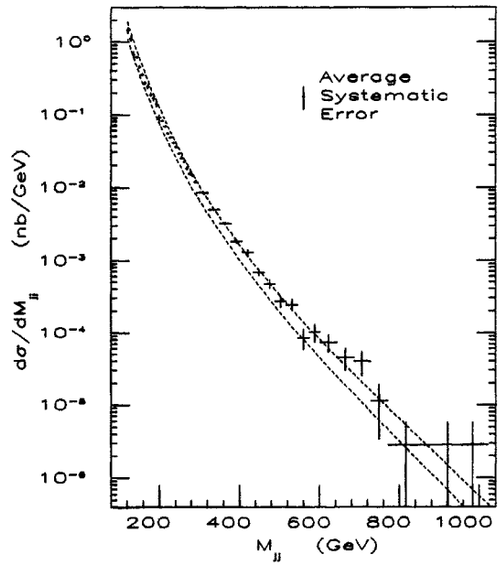

Fig. 5 M_{jj} spectrum (CDF preliminary).

experimental points with their statistical errors. The two dashed lines define a band of uncertainty in the theory, obtained as the envelope of different predictions varying the Q^2 in the range $0.5P_t^2 < Q^2 < 2P_t^2$ and using different parametrizations for the structure functions,

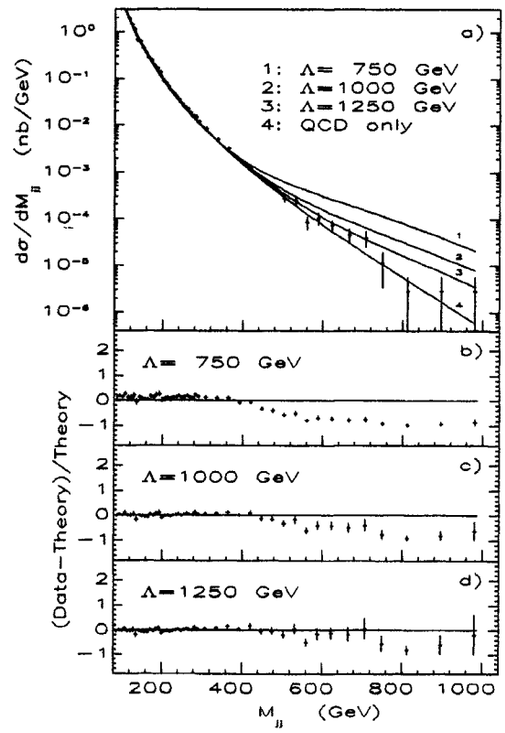

Fig. 6 M_{jj} spectrum compared to the theoretical predictions for different compositeness scales. Fig. b, c, and d show the ratios (Data-Theory)/Theory (CDF preliminary).

To illustrate the sensitivity of the mass spectrum to the quark compositeness, fig. 6a shows the data with the predicted cross sections for different values of the compositeness scale Λ. Since both data and theory have a normalization uncertainty, we normalized the theoretical predictions on the data by fitting a global normalization factor. Fig. 6b,c,d show, on linear scales, the quantities (Data-Theory)/Theory.

Both angular distribution and M_{jj} spectrum are consistent with the present CDF limit of $\Lambda > 950$ GeV. The systematic error is to be included before giving the new limit.

THREE JET EVENTS

We adopt the same conventions used by UA1 [9] to describe three jet events in the center of mass frame. As shown in fig. 7 we label the three jets with numbers 3 to 5 according to decreasing energy, reserving numbers 1 and 2 for the initial state partons.

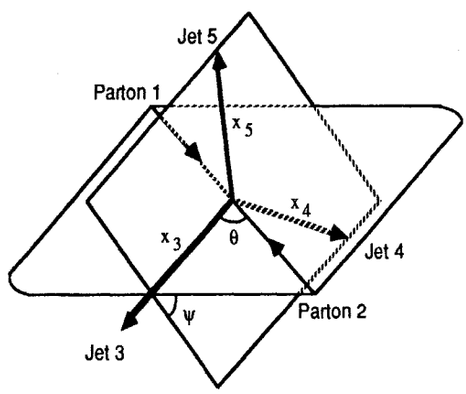

Fig. 7 Kinematics and labelling of three-jet events.

Then we define the energy fractions of the three jets $x_i = 2E_i/M_{3j}$ (where M_{3j} is the three jet invariant mass) and three angles: θ as the angle between jet 3 and parton 1, ψ as the angle between the event plane and the plane of jet 3 and parton 1, and φ as the azimuth of jet 3.

The angle φ is of little dynamical interest because of the simmetry around the beam axis. For a pure phase space decay, i.e. constant matrix element, the differential cross section $d^4\sigma/dx_3dx_4d(\cos\theta)d\psi$ is constant at fixed M_{3j}. The purpose of the analysis is to put into evidence the decay dynamics by detecting departures from the

pure phase space behavior.

Three jet events are selected by requiring at least three calorimetric clusters with $E_t > 10$ GeV and $|\eta| < 3.5$. In addition, M_{3j} is required to be greater than 200 GeV. Additional cuts are imposed to ensure that the jets are well separated from each other and from the beam: $x_3 < 0.9$, $|\cos\theta| < 0.7$, $0° < |\psi| < 150°$. This is to avoid problems both in theoretical calculations (infrared divergencies) and in measurement (inefficiency, beam jets).

The measured distributions of x_3 and x_4, with their statistical errors, are compared in fig. 8 to phase space (dashed lines) and leading QCD $2 \rightarrow 3$ predictions (solid lines). The data agree with QCD and are inconsistent with pure phase space. Fig. 9 shows the angular distributions. The error bars on the data points represent the statistical errors, the histograms represent the QCD predictions smeared with detector effects.

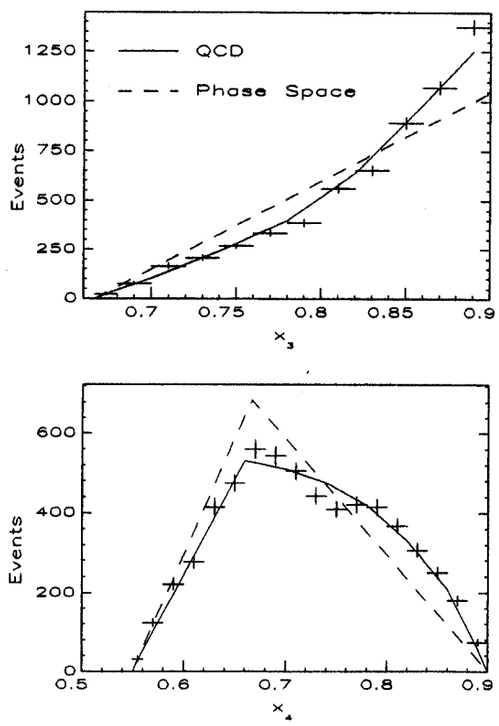

Fig. 8 Distributions of the jet energy fractions x_3 and x_4 for three-jet events (CDF preliminary).

The distribution of $\cos\theta$ closely matches the QCD prediction. The distribution of ψ also matches the QCD, but not as well. Systematic studies are underway to determine whether this small disagreement is real or an artifact of fragmentation, detector performance, and clustering algorithm.

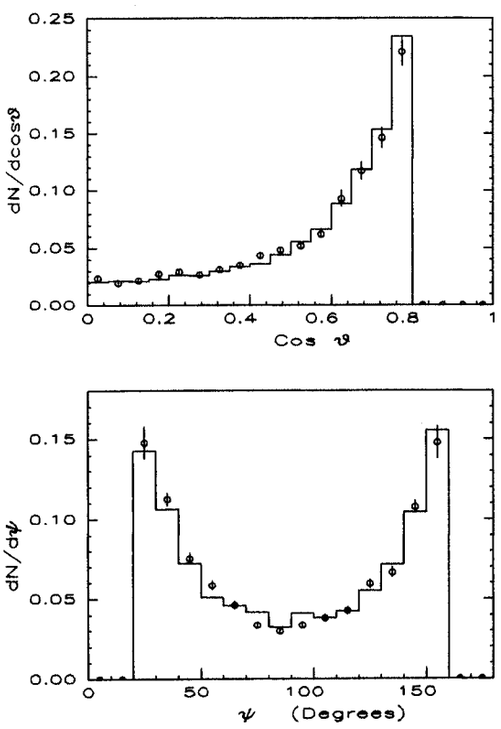

Fig. 9 Angular distributions for three-jet events (CDF preliminary).

SUMMARY

a) We measured the inclusive jet cross section $d\sigma/dE_t$ at $\sqrt{s} = 1.8$ TeV and in the Et range from 30 to 400 GeV. Investigations of the dependence of jet cross section with cone size have begun.

b) We measured the dijet angular distribution and the dijet mass spectrum.

c) We measured the energy fractions and the angular distributions of three-jet events.

d) The data appear to be consistent with both leading and next to leading order QCD predictions (where available). The spectra are sensitive to differences between structure functions. A small excess of events is observed at high E_t, over the leading order QCD prediction. Correlations in the systematic uncertainties are under study, however the previous CDF limit of 950 GeV for the quark compositeness scale Λ is still valid.

e) We have in progress detailed tests on possible structures in the mass spectrum to give limits on the axigluon mass [10] and to search for bumps, using cuts that enhance the resolution.

APPENDIX

Collaborating institutions:
Argonne National Laboratory - Brandeis University - University of Chicago - Fermi National Accelerator Laboratory - Laboratory Nazionali di Frascati of the Istituto Nazionale di Fisica Nucleare - Harvard University - University of Illinois - National Laboratory for High Energy Physics (KEK) - Lawrence Berkeley Laboratory - University of Pennsylvania - Istituto Nazionale di Fisica Nucleare, University and Scuola Normale Superiore of Pisa - Purdue University - Rockefeller University - Rutgers University - Texas A&M University - University of Tsukuba - University of Wisconsin

REFERENCES

[1] E. Eichten et al., *Rev. Mod. Phys.* **56** (1984) 579

[2] S.D. Ellis et al., *ETH-TH/90* **-3** (1990); F. Aversa et al., *LNF-90/* **012** PT (1990)

[3] CDF Collaboration, *Nucl. Instr. and Meth.* **A267** (1988) 249, 257, 272, 280, 301, 315, 330; **A268** (1988) 24, 33, 41, 46, 50, 75, 92

[4] D. Brown et al., *CDF Internal Note* **605** (1988)

[5] D. Brown et al., *CDF Internal Note* **753** (1988); S. Behrends et al., *CDF Internal Note* **1066** (1989); T. Hessing et al., *CDF Internal Note* **1131** (1990)

[6] A.D. Martin et al., *Phys. Rev.* **D37** (1988) 1161

[7] D. Duke and J. Owens, *Phys. Rev.* **D30** (1984) 49

[8] M. Dell'Orso et al., *CDF Internal note* **1056** (1989)

[9] G. Arnison et al., *Phys. Lett.* **B158** (1985) 494

[10] P.H. Frampton and S.L. Glashow, *Phys. Lett.* **B190** (1987) 157

DISCUSSION

Q. **L. Camilleri** *(CERN)*: Do you have a theoretical prediction without the 3-gluon vertex to compare to your single jet cross section?

A. **M. Dell'Orso**: No. Naively I would say that the cross-section would be about a factor of 2 lower. But I think that refitting of the structure functions (gluons), re-evaluation of $\alpha_s(Q^2)$ etc. should be redone in the new framework.

D. E. Soper *(Univ. Oregon)*: In response to Camilleri's and Dell'Orso's questions, yes, a long analysis would have to be performed in order to really compare the jet data with an "abelian QCD" theory. However, at $E_T < 50$ GeV, most of the cross section comes from gluon-gluon scattering, which would not be there in the absence of the triple-gluon vertex. (Much of it is also due to gluon-quark scattering, which also involves the triple-gluon vertex.) Thus, the cross section would be drastically altered in "abelian QCD". The agreement of the data with QCD demonstrates, I think, the existence of the triple-gluon vertex without much need for a long analysis.

Q. **L. Camilleri** *(CERN)*: a) The excess at high E_T in the single jet cross section does not seem to be reflected in the m_{jj} plot. Is this so?
b) Do you make any requirement on the away side in the single-jet cross-section?

A. **M. Dell'Orso**: a) Perhaps not.
b) No. But no monojets are seen in the high E_T region.

Q. **E. A. Gotsman** *(Tel Aviv Univ.)*: You seemed to use different values of the scaling variable Q^2 in the fits, sometimes $Q^2 = \frac{1}{2}P_T^2$, sometimes $Q^2 = P_t^2$, why?

A. **M. Dell'Orso**: We used $Q^2 = \frac{1}{2}P_T^2$ always, as it seems to give best fit to the data. The figure with $Q^2 = P_t^2$ was used just for illustrative purposes.

ENERGY FLOW AND TRANSVERSE MOMENTUM OF HADRON JETS PRODUCED IN DEEP INELASTIC MUON SCATTERING

H. J. Lubatti*
Department of Physics FM-15
University of Washington
Seattle, WA 98195 USA

ABSTRACT

Forward di-jet production observed in μp and μd interactions (Fermilab E665) is reported. The W^2 range studied, $100 < W^2 < 900$ GeV^2, is the largest yet achieved. Results from separate analyses, one using only charged hadrons and the other using both charged and the neutral energy deposited in the EM calorimeter, are presented. Correlations with $\Sigma|P_T| \simeq E_T$, an event variable, are studied. An azimuthal asymmetry of the hadrons about the virtual photon is observed.

Introduction

In the quark-parton model, deep inelastic scattering is described by virtual photon-quark scattering (Fig. 1a). The subsequent hadronization of the quark gives rise to a jet of hadrons which propagate along the direction of the parent quark with limited transverse momentum. The lowest order QCD corrections to the one-photon exchange diagram, gluon bremsstrahlung (Fig. 1b,c) and photon-gluon fusion (Fig. 1d,e) can result in final states with two forward partons each of which will fragment into hadron jets with the result that the transverse momentum of the hadrons with respect to the virtual photon direction increases.

Explicit calculations of the lowest order QCD corrections show that the average transverse momentum with respect to the virtual photon should increase with W^2 [1] with little or no dependence on other muon vertex variables. Since the virtual photon and the $q\bar{q}$ or qg pair lie in a plane (the hadronic event plane), the component of a hadron's transverse momentum that lies in the event plane ($P_{T,IN}$) should grow with W^2 whereas the component of the hadron's transverse momentum that is perpendicular to the event plane ($P_{T,OUT}$) should not depend on W^2. Further, calculations of the diagrams of Figures 1b,c by Georgi and Politzer have shown that the azimuthal distribution of hadrons about the virtual photon should be asymmetric, with the hadrons preferring to be opposite the muon [2]. Cahn has pointed out that such a correlation also arises naturally from the intrinsic transverse momentum of the partons [3].

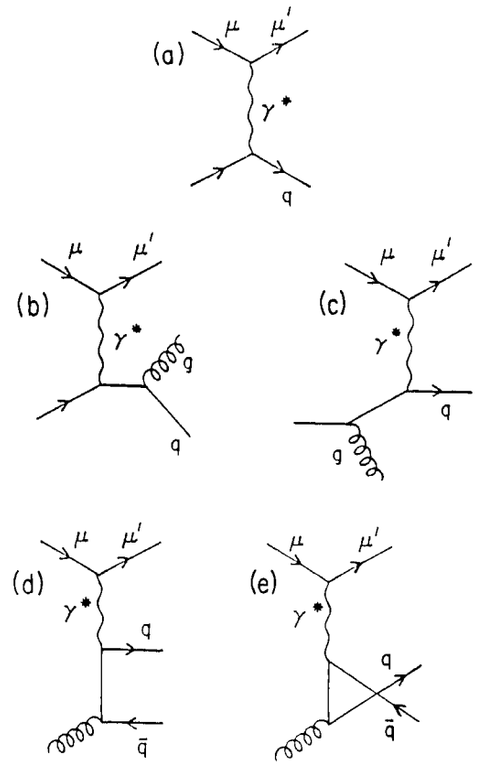

Figure 1: One photon exchange (a) and lowest order corrections; b,c): Gluon bremsstrahlung; d,e): Photon-gluon fusion.

The increase of transverse momentum with W^2 and the azimuthal asymmetry have been observed for both μN and νN deep inelastic scattering [4]. E665 by virtue of its 490 GeV/c beam extends the W^2 range of the existing data by approximately a factor of two.

Results

The data reported here were obtained during Fermilab's 1987-88 Fixed Target run with a 490 GeV/c muon beam incident upon deuterium and hydrogen targets. The ratio of μd to μp events is approximately 3:1. E665 employs an open geometry spectrometer which is described in ref. [5]. The data used for this analysis consist of hadrons with $x_F = 2P_L^*/W > 0$. The momentum of the charged tracks is measured in the forward spectrometer. The neutral energy is obtained from the electromagnetic calorimeter. The incident muon momentum is determined by the beam spectrometer to 0.5% and the scattered muon momentum is determined to 2.5% at 490 GeV/c. Typical hadron momenta are determined to a few percent. For the data shown only charged hadrons with $\Delta P/P < 5\%$ are included. The trigger used for these data is the Large Angle Trigger (LAT) which requires the detection of the scattered muon behind the hadron absorber outside of the beam region.

We first present results which include only charged hadrons. We begin by comparing to transverse momentum distributions obtained by the EMC at lower incident muon energies [6]. All transverse momenta are measured with respect to the virtual photon direction. Figure 2 compares distributions of $\Sigma P_{T,IN}^2$ and $\Sigma P_{T,OUT}^2$. The event plane is defined to be the plane where $\Sigma P_{T,IN}^2$ is a maximum. The same kinematic cuts as used by the EMC are applied to our data: $Q^2 > 4$ GeV^2/c^2, $20 < \nu < 260$ GeV, $0.1 < Y_{Bj} < 0.9$, $X_{Bj} > 0.01$, and $100 < W^2 < 400$ GeV^2. Within the statistical significance of the data agreement is good. We also find (not shown) that the fragmentation function $(1/N_\mu)dN^\pm/dz$ agrees well with EMC results.

Note that the event plane defined above becomes an experimental definition of the plane formed by the virtual photon and the $q\bar{q}$ or qg pair. Further, the $P_{T,OUT}$ distribution may be used as a measure of the single jet transverse momentum distribution since the $P_{T,OUT}$ distribution will be the same for one-jet and two-jet events.

In the following analysis we restrict ourselves to events with charged hadrons with the following selection criteria: $60 < \nu < 500$ GeV, $Q^2 > 3.0$ GeV^2/c^2, $0.1 < Y_{Bj} < 0.85$, $100 < W^2 < 900$ GeV^2, $x_F > 0$, $n_{ch} \geq 4$, $P_{charge\ track} > 8.0$ GeV/c. After these cuts we are left with a sample of 4262 μd events and 932 μp events.

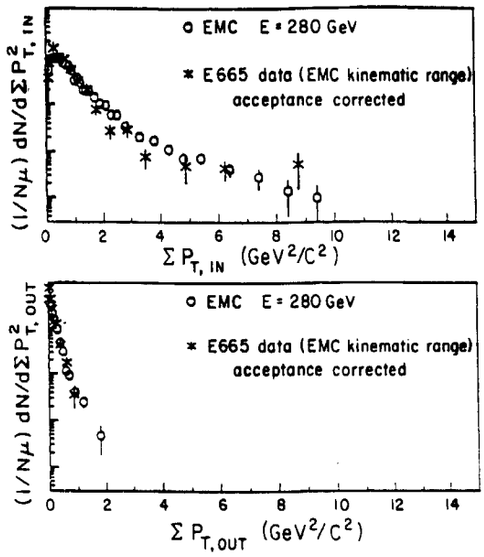

Figure 2: Normalized $\Sigma P_{T,IN}^2$ and $\Sigma P_{T,OUT}^2$ distributions compared with EMC results.

The results are compared to LUND Monte Carlo calculations [7]. We use Lepto version 5.2 [8] to simulate lepton-nucleon scattering and Jet Set 6.3 [9] to simulate the hadron fragmentation. We also compare our results to the predictions of Ariadne 3.0 [10], which simulates color dipole radiation. For all acceptance calculations we use Jet Set 4.3. We have used the Morfin-Tung [11] parton distributions except where noted. The average transverse momentum squared vs. x_F (the seagull plot) is compared with LUND model predictions in Figure [3].

It is expected that $q\bar{q}$ and qg events will have increased total transverse energy or $\Sigma|P_T|$, where P_T is the momentum of the hadron in the plane perpendicular to the virtual photon. $\Sigma|P_T|$ has a well behaved perturbative expansion (see for example ref. [12]). The single forward jet events (Fig. 1a) have hadrons with P_T distributed symmetrically in the transverse momentum plane while the two-jet events (Fig. 1b-e) would have a non-symmetric distribution. This suggests a variable which can be used to select events with large transverse energy and therefore with increased probability of containing $q\bar{q}$ or qg jets.

The event variable we use is an extension of $\Sigma|P_T|$. It was first introduced by Ballagh, *et al.* [13]. Because a single jet has a uniform P_T distribution with a most probable value P_{T0}, the distribution in $\Pi_F = A\Sigma(|P_T| - P_{T0})/\sqrt{n_F}$ is approximately a

random walk of n_F steps from the origin with width of 1, independent of multiplicity (n_F is the number of forward hadrons in the event). A is chosen to give $< \Pi_F^2 > \simeq 1$. We use $P_{T^0} = 0.32$ GeV/c and $A = 4.0$ consistent with Ballagh, *et al.*

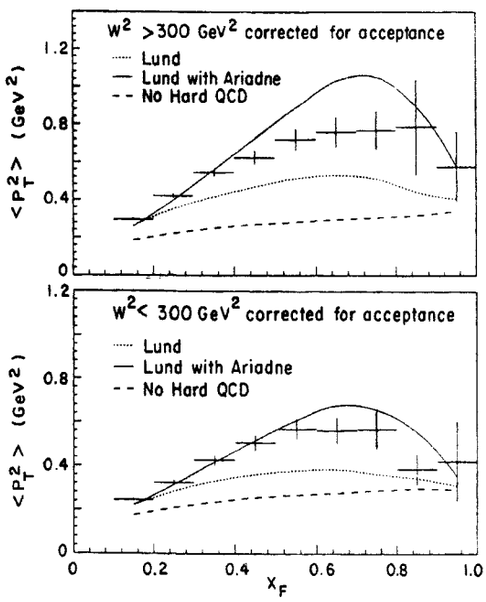

Figure 3: Average P_T^2 vs. x_F for different W^2 ranges.

In addition we define a quantity called planarity $\underline{P} = \Sigma(P_{T,IN}^2 - P_{T,OUT}^2)/\Sigma(P_{T,IN}^2 + P_{T,OUT}^2)$ where $P_{T,IN}$ and $P_{T,OUT}$ are the components of the hadron's transverse momentum lying in and out of the event plane, respectively. The scatter plot of Π_F vs. $\underline{P}$ for $W^2 > 300$ GeV^2 is shown in Figure 4 where data (Fig. 4a) are compared to the LUND Monte Carlo [11] with (Fig. 4b) and without (Fig. 4c) forward di-jet events (with diagrams 1b-1e turned on and off). The expected enhancement of planar events (large $\underline{P}$) with large Π_F is apparent in both the data and LUND with hard QCD, whereas the LUND with only single quark jets (Fig. 1a) has no events in this region. We also observe that the number of events with both large Π_F and large planarity increases with W^2, in qualitative agreement with perturbative QCD expectations.

The average multiplicity per unit P_T^2 for events with $n_{ch} \geq 4$ is shown in Figure 5 for $W^2 > 300$ GeV^2. As expected, there are considerably more hadrons with large P_T^2 for $\Pi > 3.0$ and $\underline{P} > 0.5$ whereas for $\Pi_F < 3.0$ or $\underline{P} < 0.5$ the P_T^2 distribution decreases much faster. The curves are the predictions of the LUND Monte Carlo [7] with similar cuts. The dotted curve is the LUND prediction with only single jet production.

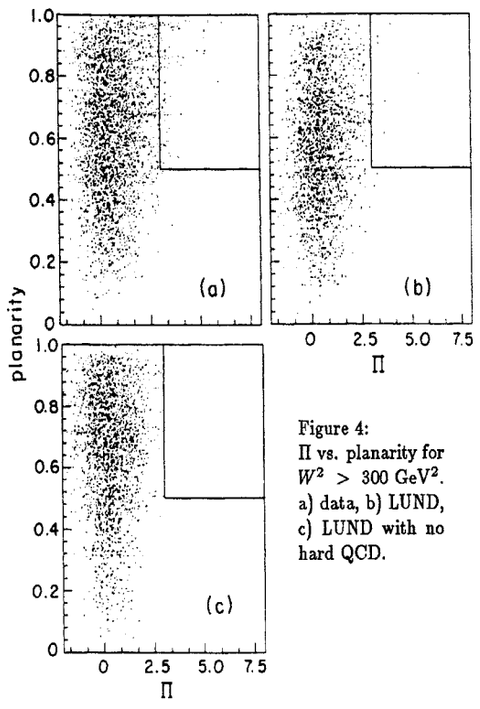

Figure 4:
Π vs. planarity for $W^2 > 300$ GeV^2.
a) data, b) LUND,
c) LUND with no hard QCD.

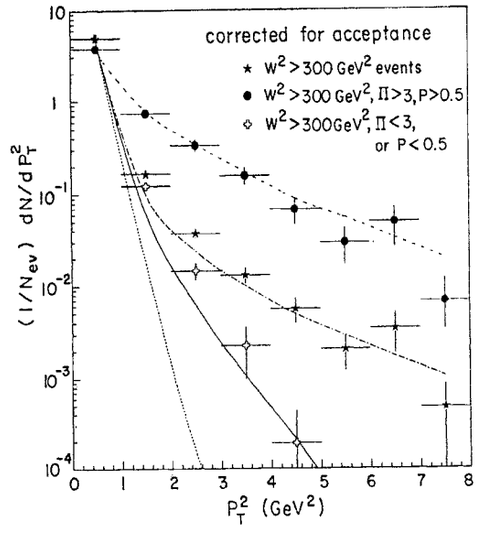

Figure 5: The average charged particle multiplicity per unit P_T^2 for $n_{ch} \geq 4$.

The scaled angular energy flow $d < E/W > /d\theta$ in the photon-nucleon center of mass system projected onto the event plane is given in Figure 6 for several Π_F regions and $\underline{P} > 0.5$. The curves are LUND model predictions. In these dis-

tributions the orientation is such that the scattered muon projected onto the event plane lies at $\theta < 0$. In each case the distributions are normalized to the number of events which pass the $\underline{P}$ and Π_F cuts. The di-jet behavior expected from the lowest order QCD corrections at large Π_F is evident and is in qualitative agreement with the LUND model.

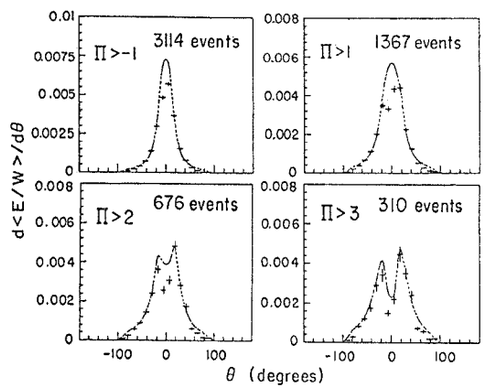

Figure 6: The angular energy flow for $W^2 > 300$ GeV^2. Curves are LUND model predictions.

We conclude from the above results that we are observing di-jet events in the forward region and that these events are, as expected from perturbative QCD calculations, associated with large transverse momentum.

In Figure 7 the azimuthal distribution, ϕ, of hadrons about the virtual γ direction is given for $\Pi_F < 1$ and $\Pi_F > 1$ for the selection $x_F > 0.2$. The $\Pi_F < 1$ distribution is consistent with little or no asymmetry, while the large values of Π_F show a significant asymmetry. The data were fit to $A + B\ cos\ \phi + C\ cos(2\phi) + D\ sin\ \phi$. For $\Pi_F < 1$ we also obtain a good fit, χ^2/DF=1.15, for an isotropic distribution ($(1/N_{ev})dN/d\phi = A$). We also observe an increase of the asymmetry as a function of x_F and P_T^2 consistent with previous results [4].

Thus far we have not made use of the electromagnetic shower energy observed in the calorimeter. We now add the electromagnetic shower energy, which allows us to include events with $n_{ch} < 4$, for our energy flow studies. Data with the EM calorimeter are only available for approximately 1/3 of the μd events. Thus in this sample we have approximately an equal number of μd and μp events. The data presented below lie in the kinematic range $0.01 < Y_{Bj} < 0.85$, $0.003 < X_{Bj} < 1.0$, $Q^2 > 3.0$ GeV^2/c^2, and $W^2 > 400$ GeV^2.

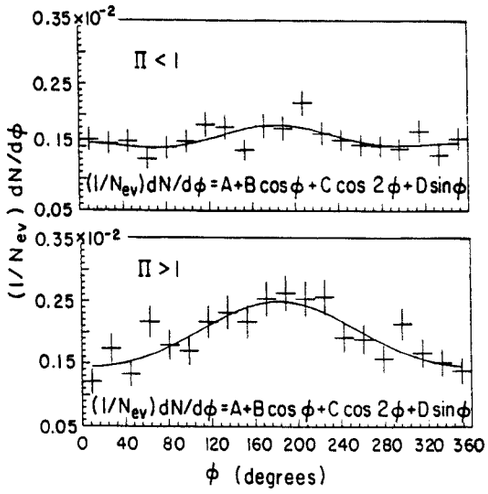

Figure 7: Azimuthal distribution of charged hadrons about the virtual γ directions (the scattered muon is at $\phi = 0°$).

We now apply a clustering algorithm to define two jets. Particles are divided into two sets on each side of the virtual photon in the event plane, and the momenta combined vectorially to yield two jet vectors. The component of momentum of each particle relative to each of these "jet axes" is calculated and particles are reassigned to the "jet axis" which yields the minimum P_T. This step is repeated three times beyond which Monte Carlo studies show that there is no significant reassignment of particles. Having thus defined the two forward jet axes we can enhance the fraction of di-jet events by selecting on the opening between the two jets (Θ_{jj}), the angle between the jet axis and virtual photon ($\Theta_{\gamma j}$), and the relative magnitude of the momenta of the jets, P_S and P_L for the smaller and larger jet momenta, respectively. The jet selection criteria we use are: $cos\ \Theta_{jj} < 0.7$, $cos\ \Theta_{\gamma j} < 0.98$, and $P_S/P_L > 0.25$.

The scaled angular energy flow in the event plane relative to the higher momentum jet axis with the lower momentum jet at positive angles is shown in Figure 8. With this jet cut, the events tend to be asymmetric in momentum. The data have been corrected for acceptance in each case. The calculations with the LUND Monte Carlo (Jet Set 4.3) using the Morfin-Tung [11] structure functions give results which are consistent with the data when hard QCD is included. The LUND curves include simulations with the GHR structure functions [14] where the main difference between reference [11] and [14] is in the gluon distribution. The Morfin-Tung distributions have much more glue at small X_{Bj} and

correspondingly less at high X_{Bj} than do the GHR distributions.

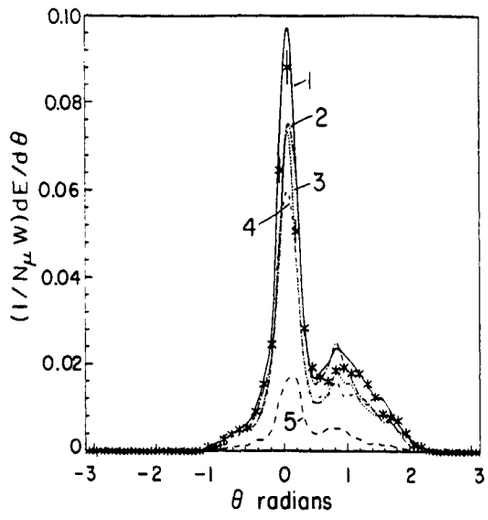

Figure 8: Scaled energy flow normalized to the number of scattered muons about the high and low momentum jet axis using charged hadrons and neutral energy. LUND model predictions: 1) Morfin-Tung structure functions, 2) No hard QCD but increased fragmentation P_T, 3) GHR structure functions with soft gluons, 4) GHR structure functions, 5) No hard QCD.

References

1. G. Altarelli and G. Martinelli, *Phys. Lett.*, **76B** (1978) 89.
2. H. Georgi and H. D. Politzer, *Phys. Rev. Lett.*, **40D** (1978) 3.
3. R. N. Cahn, *Phys. Lett.*, **78B** (1978) 269.
4. H. G. Ballagh, *et al.*, *Phys. Rev.*, **40D** (1989) 2764.
   M. Arnedo, *et al.*, *Z. Phys.* **34C** (1987) 277.
   J. J. Aubert, *et al.*, *Phys. Lett.* **130B** (1983) 118.
5. M. R. Adams, *et al.*, *Nucl. Instr. Meth.*, **291A** (1990) 533.
6. M. Arnedo, *et al.*, *Z. Phys.* **36C** (1987) 527.
7. G. Ingelman and T. Sjostrand, The Lund Monte Carlo Programs, CERN Pool Programs W5035 and W5046 long writeup (1987).
8. G. Ingleman, "Lepto Version 5.2: The Lund Monte Carlo for Deep Inelastic Lepton-Nucleon Scattering," program manual (1987).
9. T. Sjostrand, *et al.*, LU TP 86-22, October 1986.
10. B. Anderson, *et al.*, *Z. Phys.* **43C** (1989) 625.
11. J. Morfin and W. Tung, Fermilab-Pub-90/74, April 1990, to be published.
12. H. Georgi and J. Sheiman, *Phys. Rev.*, **20D** (1979) 20.
13. H. G. Ballagh, *et al.*, *Phys. Rev. Lett.*, **47** (1981) 556.
14. M. Gluck, *et al.*, *Z. Phys.* **13C** (1982) 119.

*Representing **E665**: M. R. Adams[7], S. Aid[8], P. L. Anthony[9], M. D. Baker[9], J. Bartlett[4], A. A. Bhatti[11], H. M. Braun[12], T. H. Burnett[11], W. Busza[9], J. M. Conrad[6], R. Davisson[11], G. Coutrakon[4], S. K. Dhawan[13], I. Derado[10], W. Dougherty[11], T. Dreyer[5], V. Eckardt[10], U. Ecker[12], M. Erdmann[5], A. Eskreys[3], J. Figuel[3], H. J. Gebauer[10], D. F. Geesaman[1], R. Gilman[1], M. C. Green[1], J. Haas[5], D. Hantke[10], C. Halliwell[7], J. Hanlon[4], V. W. Hughes[13], H. E. Jackson[1], D. Jaffe[7], G. Jancso[10], D. M. Jansen[11], S. Kaufman[1], R. D. Kennedy[2], T. Kirk[4], H. G. E. Kobrak[2], S. Krzywdzinski[4], S. Kunori[8], J. J. Lord[11], H. J. Lubatti[11], T. Lyons[9], D. McLeod[7], S. Magill[7], P. Malecki[3], A. Manz[10], H. Melanson[4], D. G. Michael[6], W. Mohr[5], H. E. Montgomery[4], J. G. Morfin[4], R. B. Nickerson[6], S. O'Day[8], L. Osborne[9], B. Pawlik[3], F. M. Pipkin[6], E. J. Ramberg[8], A. Röser[12], J. Ryan[9], A. Salvarani[2], M. Schmitt[6], N. Schmitz[10], K. P. Schüler[13], H. J. Seyerlein[10], A. Skuja[8], G. Snow[8], S. Söldner-Rembold[10], P. H. Steinberg[8], H. E. Stier[5], P. Stopa[3], R. A. Swanson[2], S. Tentindo-Repond[1], H.-J. Trost[1], H. Venkataramania[13], J. Wilkes[11], R. Wilson[6], M. Wilhelm[5], W. Wittek[10], S. A. Wolbers[4], T. Zhao[11]

[1]Argonne National Laboratory, Argonne, IL USA, [2]University of California, San Diego, CA USA, [3]Institute for Nuclear Physics, Crakow, Poland, [4]Fermi National Accelerator Laboratory, Batavia, IL USA, [5]Albert-Ludwigs-Universität, Freiburg i. Br., W. Germany, [6]Harvard University, Cambridge, MA USA, [7]University of Illinois, Chicago, IL USA, [8]University of Maryland, College Park, MD USA, [9]Massachusetts Institute of Technology, Cambridge, MA USA, [10]Max-Planck-Institute, Munich, W. Germany, [11]University of Washington, Seattle, WA USA, [12]University of Wuppertal, Wuppertal, W. Germany, [13]Yale University, New Haven, CT USA

DISCUSSION

Q. **N. H. Bingham** *(UC, Berkeley)*: Would you comment on how well your Lund Monte Carlo would describe your data, if you turn off QCD, but harden the parton K_T^2 distribution assumed in order to describe the average P_T^2 of the observed hadrons?

A. **H. Lubatti**: Such a modified Lund MC will indeed describe the angular energy few observed fairly well, but it does not describe well the distributions of the components of P_T^2 in and out of the event plane (defined as that plane in which the sum of $\Sigma(P_T^{\rm proj})^2$ is maximized). The Lund model with QCD does describe these $(\Sigma P_T^{\rm in})^2$ and $(\Sigma P_T^{\rm out})^2$ distributions well.

Q. **B. Ioffe** *(ITEP, Moscow)*: Did you try to separate the two sources of the jet azimuthal asymmetry: from primordial quarks (at nonperturbative origin) and from perturbative gluons which can, in principle, be done by studying the Q^2-dependence of the asymmetry?

A. **H. Lubatti**: Our Q^2 distribution is limited to small values, so we do not have much range and our data sample is limited; however, your point is well taken and we will re-examine the Q^2 dependence.

Q. **E. Tsyganov** *(JINR)*: When you tried different algorithms for the jet selection, have you ever tried the algothrims proposed by Prof. A. Baldin from Dubna? In this algorithm jets are considered as clusters in 4-velocity space. It is especially good for small q-square jets, as in your case. Besides, these variables are Lorentz-invariant.

A. **H. Lubatti**: Unfortunately I only recently (at this conference) became aware of Prof. Baldin's paper. It looks like a very promising approach which may be very useful to us.

PRODUCTION OF HIGH-p_t JETS IN HADRON-NUCLEUS COLLISIONS

A. Zieminski
Indiana University, Bloomington, IN 47405

ABSTRACT

Experimental and theoretical aspects of jet production in hadron-nucleus collisions are discussed. Recent data from Fermilab experiments studying production of single high-p_t hadrons, high-p_t hadronic pairs and "jet-like" clusters are summarized. The data at the highest available energies are consistent with the A^α parametrization for the nuclear dependence of the cross-sections, with the value of α within 0.10 from unity.

1. Introduction

In the present review we shall concentrate on hadroproduction of jets.[11] The main questions of interest are: how do partons propagate through nuclear matter to and from a hard interaction ? Is there any evidence for their energy attenuation and/or for partons' multiple scattering? Is there evidence for nuclear shadowing and/or broadening of jets with atomic weight A? Are the results from experiments using limited aperture calorimeter triggers compatible with those triggering on single hadrons or hadron pairs? We shall review the experimental data from this qualitative point of view. A more quantitative comparison with QCD model predictions is rather premature at this stage of the data accuracy and the sensitivity of model predictions.

The new data on hadroproduction of jets come from Fermilab experiments studying pA collisions at the c.m. energies, $\sqrt{s}$ = 27-39 GeV : E557[2] , E605[3] , E609[4,5] and E711[6,7] .

2. High-p_t inclusive hadron pair production

It was found fifteen years ago that the observed cross section for hadronic production of high-p_t single hadrons off nuclei increases with the atomic number A faster than A^1.[8] This result and results of the follow up experiments were interpreted as evidence for multiple scattering of active partons inside the nucleus, before and after a hard scattering took place. The new data[3] on pA interactions at 800 GeV/c, previously presented in Ref.[1], extend the range of p_t studied from 6 GeV/c up to 10 GeV/c. The values of α, in a cross section parametrization A^α, for a given particle type seem to decrease with the particle's p_t. The new data when compared with data recorded and lower c.m. energies indicate a clear reduction in the nuclear enhancement with energy at a fixed value of p_t.

The size of nuclear enhancement is less clear for the di-hadron production processes. The E605 Collab.[3] reports values of α slightly less than 1.0 (see Fig. 1) , whereas the E711 data[6] taken at the same incoming proton momentum and in the similar di-hadron phase space region show values of α close to 1.05 irrespectively of the di-hadron pair mass or charge combination ($< \alpha >$=1.049 $\pm$0.007$\pm$(0.025)). The two data sets are consistent within two standard deviations if one takes into account an overall relative 10 % normalization error of the E605 cross sections. The E605 Collab. has also measured the A-dependence of the variable p_{out} , which represents a transverse momentum component of the slower hadron in the direction perpendicular to the production plane, defined by the beam direction and the faster hadron momentum. The authors interpret the increase of nuclear enhancement at higher values of p_{out} (see Fig. 1) as an indication for multiple scattering. The increase is particularly strong for low mass di-hadrons. The nuclear shadowing (values of α less than one), observed in their data, could manifest the parton energy attenuation prior to the hard-interaction.

Recent phenomenological calculations by Kim and Kopeliovich took into account both: incom-

ing parton energy losses and inelastic interactions of scattered partons after they travel over a distance longer than their formation length (which depends on the parton momentum and x_T). The authors of Ref.[9] were able to reproduce majority of the available di-hadron data collected with the incoming proton momenta from 70 GeV/c to 800 GeV/c.

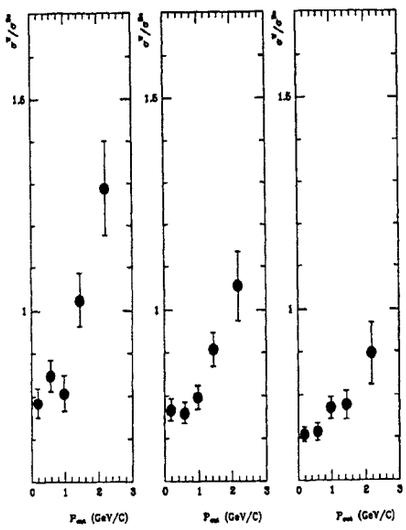

Fig. 1 Ratio of W to Be per nucleon h^+h^- pair production vs p_{out} for three di-hadron mass bands:

(a) 7.5 GeV < M < 8.5 GeV;
(b) 8.5 GeV < M < 9.5 GeV
(c) M > 9.5 GeV.

The E711 Collab.[7] combined information on high-p_t hadrons with the electromagnetic calorimeter energy deposited in cones around direction of a leading hadron. This way they estimated an average fraction of jet energy carried by the leading hadron. They claim that within experimental errors the high-p_t parton fragmentation is not affected by interactions taking place at the nuclear level.

3. Jet production

Experimentally, jets are selected by triggering on events which deposit a large amount of transverse energy in some region of phase space comparable to the anticipated jet size. The E557 Collab.[10] reported a strong A dependence of cross sections for producing events with a given E_t . The calorimeter apertures used in the trigger had a 45° - 135° coverage in the nucleon-nucleon c.m. polar angle and at least $\pi/2$ in the azimuthal angle. The values of α, in the A^α cross section parametrization, at a given E_t were larger than 1.5 for both large and small-aperture triggers. However, the authors[10] noticed that "jetty" events, selected by requiring large value of planarity, exhibit an A dependence consistent with α =1.0 - 1.1.

The planarity analysis is sensitive to both the A-dependence for the jet production rates and possible changes in the event structure with A. The E557 Collab. attempted to separate the two effects. Jets were defined as sets of particles produced in a cone of radius R in the ϕ-η space around the jet axis calculated as a vector sum of particle momenta[2]. The analysis was done for value of R = 0.85. Events were selected for which two jets were found with c.m. rapidities $|\eta^*| < 0.4$ and the sum of the transverse energies of two jets (E_t^{jj}) exceeded 13 GeV.

The transverse-momentum flows as functions of the azimuthal angle difference calculated with respect to the jet axis, are shown in Fig. 2a. The data for hydrogen exhibit clear maxima attributed to the "trigger" (higher p_t) jets and "away" jets. The carbon and lead data indicate significant smearing of the di-jet structure for nuclear targets. This is due to higher level of the underlying event for the C and Pb data, and mainly to smearing in the position in azimuth of the "away" jet around 180° for heavier nuclei.

The differences between nuclear targets are much less pronounced when events with large planarity, P > 0.85, are selected, as shown in Fig. 2b. For this sample of events, the nuclear enhancement parameter α is 1.06± 0.03, compared with α = 1.48± 0.02 for the uncut sample.

The jet acoplanarity effect is thoroughly discussed in Ref. [5]for the pA interactions at 400 GeV/c. It was found that the Pb jets are only slightly larger than those from H, their rms width in the azimuthal angle being 16±1deg and 14±1 deg, respectively (for jets with average $p_t \simeq 5$ GeV/c). Fig. 3 shows rms of the difference in azimuth between the two jet momentum vectors, $\sigma_{\Delta\Phi}$, as a function of A. The acoplanarity appears to increase smoothly with A.

The di-jet cross sections (E557 Collab.[2]) are shown as functions of E_t^{jj} in Fig. 4a. Figure 4b shows the variation of α with E_t^{jj}. Both jets were required to be within the range $-0.4 < \eta^* < 0.4$. Although the values of α are about 1.5 at E_t^{jj}= 13 GeV, they decrease at larger values of E_t^{jj}.

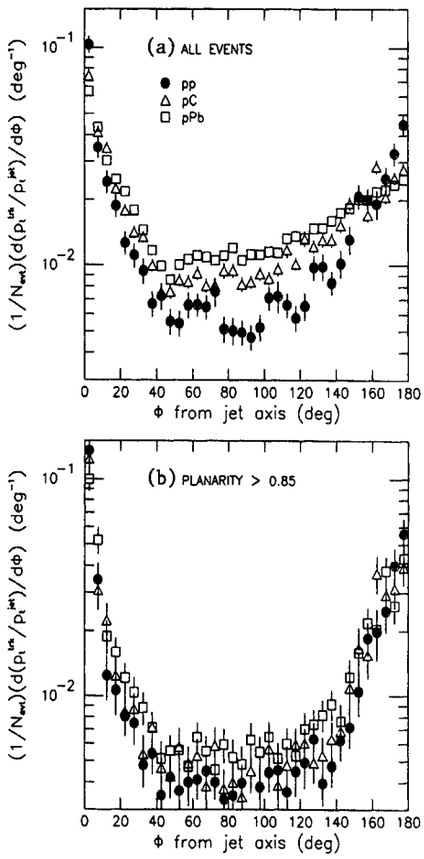

Fig. 2 Transverse-momentum flow vs the azimuthal angle relative to the "trigger" jet axis ϕ normalized to the p_t of the "trigger" jet. Data with E_t^{jj} > 13 GeV are shown. Tracks with c.m. rapidities $-1.0 < \eta^* < 1.5$ are included. (a) no planarity cut; (b) P > 0.85.

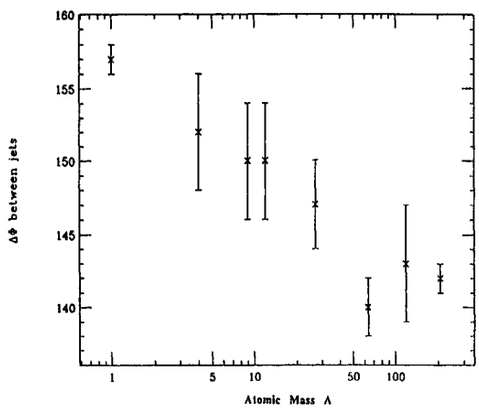

Fig. 3 The A-dependence of the distribution, the azimuthal angle between the found jet axes. The rms width of 180 deg peak in $\Delta\phi$ as a function of nuclear mass A. Data from Fermilab E609 studying pA collisions at 400 GeV/c.

The values of α, shown in Fig.4b, have not been corrected for the effect of the underlying-non-jet-event, by which we mean contributions to the energy within the jet cone from particles emerging from the target and beam jet fragmentation. The effect was estimated using the distributions similar to those presented in Fig. 2a. The transverse energy density per unit $\eta^*$and unit ϕ of the underlying event was assumed to be uniform in ϕ. The underlying event level was determined by integrating p_t from ϕ= 45° to ϕ = 90° away from the jet axis at ϕ= 0°. For the *pp* data the contribution of the underlying event to the p_t within the jet cone decreases from 20% to 9% as p_t of the clusters (R=0.85) increases from 7 GeV/c to 10 GeV/c. For heavier nuclei the level of the underlying event is significantly higher and varies with η^*. The corresponding numbers for the pPb data are: 34% to 23% variation within the $-0.3 < \eta^* < 0.3$ range at p_t = 7 GeV/c and 21% to 14% variation at p_t = 10 GeV/c. Since *pp* jet cross sections found in Ref.[2], were consistent with previous experiments, the authors corrected the data for other nuclei with respect to hydrogen and left the *pp* data intact. The corrected A-dependence of the di-jet production is displayed in Figs. 4cd. Values of α are close to unity over a large range of jet energies.

The results of the above analysis suggest that events selected by the jet algorithm are indeed due to hard-scattering, in spite of the fact that production of jets off heavy nuclei is obscured by the target fragmentation debris.

4. Jets and Target Fragmentation

The E609 Collab. measured the average laboratory energy flow into the nuclear target (η_{lab} <2.83) region, $< EB >$, for two-jet events with mean $p_t > 4$ GeV/c[4]. They computed EB for each event using: EB = 400 GeV - ECAL - BCAL, where ECAL and BCAL were defined as the total laboratory energy detected in the main and beam calorimeters, respectively. The value of $< EB >$ is 50 GeV higher for Pb data compared to H. Figure 5 shows the measured dijet event cross section parametrized in terms of A^α, as a function of EB. Figure 5 indicates that for those (rare) events with little energy transfer to the target nucleus, the di-jet production is roughly proportional to A. By contrast, much faster A dependence is observed for dijet events with substantial energy transfer to the target. This might be expected in a multiple scattering model of partons.

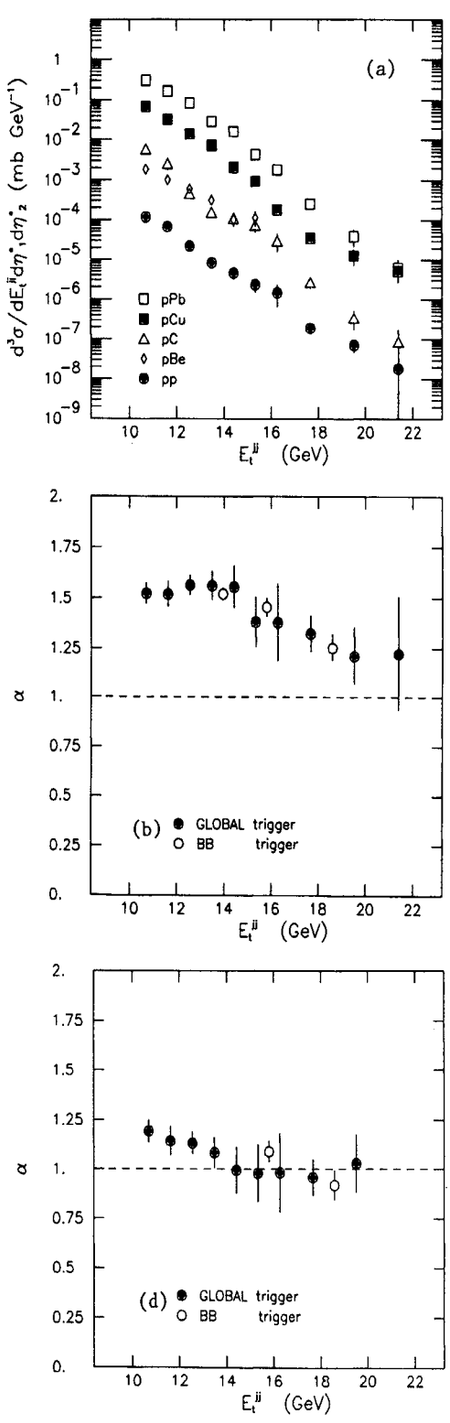

Fig. 4 (a) Dijet cross section dependence on E_t^{jj} for pA interactions at 800 GeV/c, where E_t^{jj} is the scalar sum of transverse energy of the two jets. (b) α vs E_t^{jj}; (d) Same as (b) after correction for the underlying event (see text) was applied to the heavier nuclei data (E557 results).

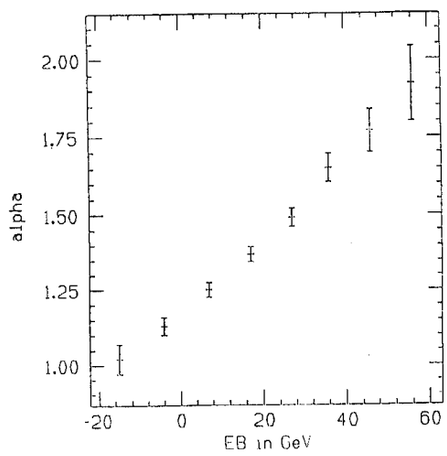

Fig. 5 A^{σ} dependence of the dijet production cross section as a function of the backward energy flow EB, where EB is the difference between incoming 400 GeV energy and the total laboratory energy detected in the main and beam calorimeters (E609

REFERENCES

1. For a recent reviews see: J. Rutherfoord, Proceedings of the 3rd Conf. on the Intersections between Particle and Nuclear Physics, Rockport, Maine, p.157(1988); A. Zieminski, Proceedings of the DPF Meeting, Storrs, Co, p. 672 (1988).
2. C. Stewart et al., *Phys. Rev.* **D42**, 1385 (1990)
3. B. Straub , PhD Thesis, Univ. of Washington (1990); J. Rutherfoord - private communication
4. R. C. Moore et al., Argonne preprint ANL-HEP-PR-98-131; Phys. Lett. B - in press
5. M. Corcoran et al. , "Evidence for Multiple Scattering of High Energy Partons in Nuclei", paper submitted to this Conference.
6. K. Streets et al., Fermilab preprint Pub-89/42-E(1989), unpublished.
7. G. Boca et al., "Average Fraction of Jet Momentum Carried by High-p_t Leading Hadrons", paper submitted to this Conference.
8. J. Cronin et al., *Phys. Rev.* **D11**, 3105 (1975) .
9. V. T. Kim and B. Z. Kopeliovich, Dubna preprint E2-89-727 (1989), Z. Physik C - in press
10. R. Gomez et al., *Phys. Rev.* **D35**, 2736 (1987)